Silicon-germanium receivers for short-waveinfrared optoelectronics and communications

Daniel Benedikovic, Léopold Virot, Guy Aubin, Jean-Michel Hartmann, Farah Amar, Xavier Le Roux, Carlos Alonso-Ramos, Éric Cassan, Delphine Marris-Morini, Jean-Marc Fédéli, et al.

Review

Daniel Benedikovic*, Léopold Virot, Guy Aubin, Jean-Michel Hartmann, Farah Amar, Xavier Le Roux, Carlos Alonso-Ramos, Éric Cassan, Delphine Marris-Morini, Jean-Marc Fédéli, Frédéric Boeuf, Bertrand Szelag and Laurent Vivien

Silicon–germanium receivers for short-wave-infrared optoelectronics and communications

High-speed silicon–germanium receivers (invited review)

https://doi.org/10.1515/nanoph-2020-0547
Received September 28, 2020; accepted November 25, 2020; published online December 8, 2020

Abstract: Integrated silicon nanophotonics has rapidly established itself as intriguing research field, whose outlets impact numerous facets of daily life. Indeed, nanophotonics has propelled many advances in optoelectronics, information and communication technologies, sensing and energy, to name a few. Silicon nanophotonics aims to deliver compact and high-performance components based on semiconductor chips leveraging mature fabrication routines already developed within the modern microelectronics. However, the silicon indirect bandgap, the centrosymmetric nature of its lattice and its wide transparency window across optical telecommunication wavebands hamper the realization of essential functionalities, including efficient light generation/amplification, fast electro-optical modulation, and reliable photodetection. Germanium, a well-established complement material in silicon chip industry, has a quasi-direct energy band structure in this wavelength domain. Germanium and its alloys are thus the most suitable candidates for active functions, i.e. bringing them to close to the silicon family of nanophotonic devices. Along with recent advances in silicon–germanium-based lasers and modulators, short-wave-infrared receivers are also key photonic chip elements to tackle cost, speed and energy consumption challenges of exponentially growing data traffics within next-generation systems and networks. Herein, we provide a detailed overview on the latest development in nanophotonic receivers based on silicon and germanium, including material processing, integration and diversity of device designs and arrangements. Our Review also emphasizes surging applications in optoelectronics and communications and concludes with challenges and perspectives potentially encountered in the foreseeable future.

Keywords: group-IV nanophotonicss; integrated optoelectronics and communications; optical photodetector.

1 Introduction

In the recent years, the appetite for data traffics was heightened by the Internet era, social networks and streaming media by continuously calling upon faster and immediate connections between Internet of Things devices [1, 2]. However, needs of emerging data-intensive areas such as next-generation wireless and optical communications [3, 4], cloud storage and servers [5], high-performance computing [6], data centers [7], among others, are now exceeding the transmission capacity of traditional copper-based interconnects [8, 9].

Optical technologies are foreseen to alleviate the interconnection bottleneck of much slower metalized electronic wires, as the former, proceed at speed of light, offer much larger bandwidth. Indeed, a growing number of optical solutions promises bountiful opportunities to be cheaper in production, faster in operation, lower in latency, higher in bandwidth, while consuming far less energy, improving both thermal and power link budgets.

***Corresponding author: Daniel Benedikovic**, Université Paris-Saclay, CNRS Centre de Nanosciences et de Nanotechnologies, 91120, Palaiseau, France; and Recently with Department Multimedia and Information-Communication Technologies, University of Žilina, 01008 Žilina, Slovakia, E-mail: daniel.benedikovic@c2n.upsaclay.fr. https://orcid.org/0000-0002-2239-0041
Léopold Virot, Jean-Michel Hartmann, Jean-Marc Fédéli and Bertrand Szelag, University Grenoble Alpes and CEA, LETI, 38054 Grenoble, France
Guy Aubin, Farah Amar, Xavier Le Roux, Carlos Alonso-Ramos, Éric Cassan, Delphine Marris-Morini and Laurent Vivien, Université Paris-Saclay, CNRS, Centre de Nanosciences et de Nanotechnologies, 91120, Palaiseau, France
Frédéric Boeuf, STMicroelectronics, Silicon Technology Development, 38923 Crolles, France

Albeit optical technologies, particularly optical fibers, have eliminated copper wires in the metro and long-haul links, and do progressively in last-mile access networks, optical concepts have not completely replaced some electronic interfaces within short-reach hierarchies [8–10].

Of special interest to next-generation systems are the points of access through Ethernet lines with electro-optical/opto-electrical interfaces and high connection throughput. As Ethernet transmission speed is migrating from 10 and 40 GE standards toward 100 GE and beyond [11–13], on-chip semiconductor nanophotonics becomes more prevalent in optical transceivers at both ends of the fiber-optic links [14]. Integrated nanophotonics, especially the branch made of crystalline group-IV semiconductors, is destined to play an essential role in modern computation, communication, and optoelectronics industries, fusing every facet of our digital life [15]. Recent breakthroughs in nanophotonics have showed a good potential to interlink electronics and photonics on single-chip circuits [16, 17], while leveraging advanced microelectronics fabrication facilities [18]. Group-IV nanophotonics holds prospects to become a multi-functional platform with monolithic integration [19, 20], potentially supporting low-cost and high-yield production at scales that enable market penetration [21]. So far, a wealth of basic building blocks has been developed, including low-loss and high-performance waveguides and devices [22, 23], silicon (Si)-based [24–26] or germanium (Ge)-based [26–28] light sources, high-speed optical modulators [29, 30], as well as photodetectors [31–33]. These achievements will likely be stepping stones to improve the performance of, and bringing novel functions to, monolithic group-IV-based platforms.

Optical photodetectors are critical components in this environment. Early developments of Ge detectors go back to 1950s – 1970s [34–36]. Photodetectors are typically positioned at the end of an optical chain to convert a signal from optical to electrical. As the scale and diversity of photodetectors depend not only on the material system but also on the targeted applications, device performance criteria can differ depending on the available fabrication/integration technologies [37]. On-chip optical receivers built upon Si and Ge semiconductors offer a set of levers to meet targets for cost-effective, bandwidth-enhanced and energy-aware applications in optoelectronics outlets as in computation and communication networks.

In this Review, we discuss recent advances in the field of group-IV photodetectors, in particular those made out of Si and Ge/Ge-based alloys. We give in Section 2 a brief classification of materials conventionally harnessed for optical photodetection and present emerging materials. Section 3 details methods for Ge growth and the status of photodetector integration with Si waveguides and Si complementary metal-oxide-semiconductor (CMOS) lines. We describe in Section 4, the core of this Review, the properties of cutting-edge Si–Ge photodetectors. We notably focus on achievements in mainstream fiber-optics spectral bands and extended communication windows, device arrangements for low-power and high-power scenarios, as well as current advances in attractive p-i-n and avalanche structures. Finally, in Section 5, we conclude with a discussion on maturity levels, challenges and prospects of chip-integrated Si–Ge photodetectors.

2 Enabling materials for photodetection

The central mechanism harnessed for light detection is to transduce impinging photons with given energy into electrical signals, typically current or voltage, which can then be collected by an electronic readout circuitry. Indeed, an efficient photon-to-electron conversion depends on the electronic bandgap of the active material used to that end [31–33]. Figure 1 shows spectral and bandgap energy dependence of the absorption coefficient for several well-known semiconductors used in optical photodetectors. Accordingly, several pure or alloyed materials are presently used in a wide variety of optical photodetectors.

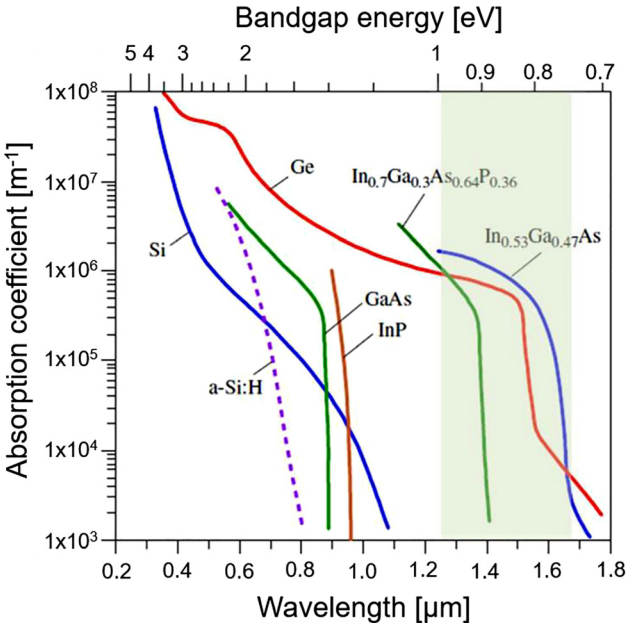

Figure 1: Absorption coefficient as a function of the wavelength and bandgap energy for several semiconductors typically harnessed in optical photodetectors. Figure adapted from a study by Virot [38].

Si is an indirect bandgap semiconductor with an energy bandgap of 1.12 eV. This hampers both efficient light emission and detection at attractive near-infrared and short-wave-infrared (SWIR) wavelengths, 1.3 and 1.55 μm. Although Si photodiodes are broadly used in the visible spectrum [39], their operation is rather limited above the indirect-band edge (1.1 μm). The energy level of NIR photons is not high enough to get over the Si bandgap, precluding an efficient generation of photo-carriers (electron-hole pairs). Si photodiodes can be found in form of p-i-n [40], avalanche [41, 42] and metal–semiconductor–metal (MSM) structures [43]. The deficiency of NIR Si diodes can be partially overcome by concepts, exploiting optical cavities [44], two-photon absorption [45], poly-Si deposition [46], or defect-assisted photo-generation [47]. Although significant effort has been dedicated to the improvement of NIR and SWIR Si photodetectors, their opto-electrical performances are currently inferior to that of other material systems.

Ge, like Si, is a crystalline semiconductor from the group-IV atomic column. Ge has proved to be an excellent complement to Si in modern electronics chips, and the same is seen in chip-scale nanophotonics. Unlike Si, Ge has a quasi-direct energy bandgap 0.8 eV. This makes Ge a very good alternative for a number of active chip functionalities [27–33, 48]. The wide transparency window of Ge is also appealing in the mid-wave-infrared and long-wave-infrared ranges [20, 49, 50]. From a light detection point of view, Ge's appeal stems from an absorption that is high enough over a wide spectral range, a fast mobility for electrons and holes, mastered epitaxy and decent crystalline film quality, seamless CMOS fabrication with foundry-enabled monolithic integration [19, 51–53]. Compared to the bulk Ge, plotted in Figure 1, the two-step Ge growth method (see Section 3 for more details) typically results in a tensile strain of about 0.2%. This helps improving the material absorption at a wavelength of 1.55 μm as well as red shifts the direct gap toward longer wavelengths [31–33, 37, 38]. Alloying Ge with Tin (Sn), a semimetal, facilitates the integration of new devices on Si chips, enabling device operation beyond the Ge cutoff wavelength [54]. While Ge is promising for a full photonic platform based on group-IV semiconductors, a few difficulties remain, such as the 4.2% lattice mismatch with Si, generating structural defects and the intrinsically high noise.

III–V compound semiconductors are, with their direct bandgap, the most mature materials for use in optically active devices. For photodetection, favorable features of III–V semiconductors are tailorable energy bandgaps, high absorption and high carrier drift velocities, as well as mature device designs and fabrication flows [55–57]. Photodiodes based on indium phosphide (InP), gallium arsenide (GaAs), indium gallium arsenide, and indium gallium arsenide phosphide are the standard bearers that have been in place for decades and dominate the markets. In the last years, integration of III–V hetero-structures with Si CMOS platforms [57, 58] picked up steam, with chip-to-chip bonding, direct hetero-epitaxy, or transfer printing methods used to that end [59–62]. Although such approaches would enable to benefit from both worlds, heterogeneous integration still faces severe challenges. This includes increased process complexity and cost, lattice mismatch, difference in thermal expansion coefficients, formation of anti-phase boundaries, or even contamination hazards in Si CMOS foundries.

In parallel with advances in crystalline semiconductor photodetectors [39–47, 51–63], new material classes and integration strategies were shown to have great potentials in integrated nanophotonics. Emerging photodetector designs include plasmonics [64–69] and two-dimensional (2D) materials such as graphene [70–73] or transition metal dichalcogenides [74–79], among others studied alternatives [80–86]. Such materials and concepts are attractive for future on-chip photodetection due to their compactness (atomic-layer thicknesses for 2D materials or short structures for plasmonics), versatile electrical and optical properties, and strong interactions between light and matter [66, 71, 75]. The stacking and merging of those materials with many CMOS-compliant photonic platforms [64–79], including Si, Ge, silicon nitride (SiN), or titanium nitride, would be appealing. This hybrid or quasi-monolithic integration may happen without additional process intricacies or needs to match crystal lattices as in Si–Ge [31–33] or III–V-on-Si [58, 60, 61, 63] devices. Whereas integration can be facilitated by fabless chip manufacturing [18, 19] and improved wafer-level transfer/growth methods for 2D materials [71, 72], the van der Walls nature of such 2D materials may minimize surface defects [71, 73]. Typical examples are, but not limited to, Si photodetectors with plasmonics and graphene [64], Ge-plasmonic waveguide photodetectors [67, 68], metal–graphene–metal photoconductive photodetector on Si substrate [69], $MoTe_2$-based photodetectors with Si waveguide integration [75], graphene–$MoTe_2$–metal photodetectors stacked on Si waveguides [79], MoS_2-based photodetectors in a SiN photonic circuit [77], or devices exploiting $MoTe_2$–graphene-based heterostructure [78]. Such detectors progressed rapidly in the last few years, with smaller device footprints, broader spectral photo-responses, and better speeds. They are still at an early development stage, however [66, 72–74]. We will not detail more in depth the performances of such material systems, as they are covered

in dedicated reports and reviews. Instead, in the rest of this Review, we will focus on state-of-the-art Si–Ge photodetectors.

3 Processing matters and integration status

Si and Ge are mainstream materials in fields of electronics and nanophotonics [87]. Growing pure Ge directly on Si is desirable for the fabrication of Si–Ge photodetectors. However, the growth of Ge films on Si is not easy as the lattice mismatch between these two materials is large, 4.2% (a_{Si} = 5.431 Å, to be compared with a_{Ge} = 5.658 Å). This results in a high density of misfit and threading dislocations in the Ge layer, and potentially, a high surface roughness. The later may prevent the fabrication of Ge devices in Si CMOS facilities. Meanwhile, dislocations have a significant impact on device performance such as dark-current increase and carrier mobility decrease.

3.1 Germanium growth techniques

First approaches to growing good Ge films dates back to the 1980s and 1990s [88–91]. Optimized graded SiGe buffers were used to reduce the amount of threading dislocations in the Ge films on top. Graded SiGe buffers call upon rather thick layers to obtain high quality moderate [88–90] and/or high Ge content [91] in films on top. Recent Si photonics devices require Ge detectors close to Si waveguides to have an efficient connection between them [92], precluding the use of such graded SiGe buffers. Ge has thus to grown directly on Si, with two-step deposition technique to mitigate the impact of the 4.2% lattice mismatch between those semiconductors. The two-step approach avoids islanding during chemical vapor deposition (CVD) process [93–97] and yields rather smooth, high quality Ge layers, in the end. A thin Ge "seed" layer is first of all grown at low temperature, typically in the ~320–450 °C range. The vast majority of the lattice mismatch is accommodated in it, with the formation of a regular array of edge misfit dislocations ~10 nm apart, without too much surface roughening because of elastic strain relaxation. In the second step, high-temperatures, ranging between ~600 and 850 °C, are leveraged to grow faster a Ge layer with a much better crystalline quality. To further reduce the amount of threading dislocations in the Ge films and reach values around 10^7 cm^{-2}, post-growth thermal cycling at high-temperatures can be used. Different alternatives for high-quality Ge films have been explored over the course of years. This includes combined approach, where sub-micron SiGe buffered layers are used before the two-step growth technique [98, 99], direct Ge growth with additional H_2 annealing [100, 101], low-energy plasma-enhanced CVD to reduce the overall thermal budget [102], or selective epitaxial growth (SEG) in etched Si recesses [103] (shown in Figure 2). Indeed, SEG is better suited to integrate Ge devices at discrete location in a Si CMOS circuit [104]. This, in turn, facilitates the entire process flow within nanophotonics foundries. For further details on Ge growth techniques and methods, not only limited to Ge photodetectors, we refer readers to dedicated sources [87, 103, 105].

3.2 Waveguide and CMOS-compliant integration

High-performance Si–Ge photodetectors were initially designed as discrete normal-incidence devices, favoring fiber-optic or free-space light coupling. Despite many advances in the last decades [107–112], optical photodetectors with a normal-incidence showed more shortcomings than advantages. Indeed, very thick absorbing layers are typically required to efficiently capture the incident light. This, in turn, results in large device footprints, higher dark currents and capacitance, and limited responsivity-bandwidth product. All of this limits the achievable device speed and sensitivity. Such a balance in photodetector performances can be addressed by Ge photodetectors integrated directly with Si waveguides.

Waveguide-integrated detectors are, indeed, more appealing for chip-scale nanophotonics than their free-

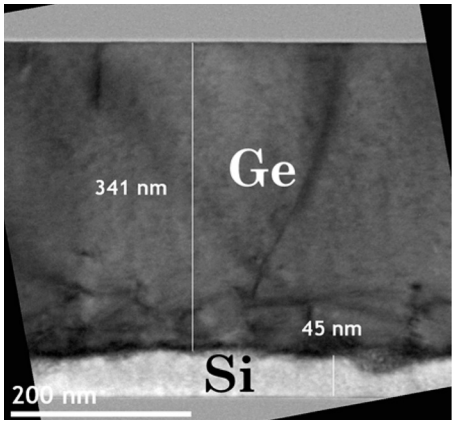

Figure 2: Cross-sectional transmission electron microscopy image of a Si cavity after Ge epitaxial growth and chemical mechanical polishing steps. Figure adapted with permission from a study by Virot et al. [106] © Chinese Laser Press.

space counterparts. Waveguide-integrated photodetectors have smaller active device areas, facilitating low-noise operation with an improved sensitivity. They are also better suited to mature Si CMOS fabrication lines. With a waveguide integration, the collection path of generated photocarriers and the light propagation path are orthogonal to each other, which is a major advantage over normal-incidence devices. The waveguide design yields a new degree of freedom to optimize responsivity and bandwidth almost independently, i.e. the device speed is not compromised by its photo-response. Seminal work by Ahn et al. [113] on the waveguide-integrated detector showed those advantages. They demonstrated first vertical hetero-junction diodes, achieving a maximum responsivity at 0 V. Since then, integrated optical photodetectors based on Si–Ge platforms were extensively investigated, with a great number of device arrangements assessed since Ahn et al. pioneering work [114–118].

In order to inject light in integrated Ge photodetectors, evanescent-coupling [115, 116, 119] or butt-coupling [117] with Si waveguides are typically used. Waveguide-photodetector coupling configurations are shown in Figure 3. For an evanescent-coupling of light, we can distinguish (i) the top-to-down scheme [111], where the waveguide is positioned on top of the Ge photodetector (Figure 3(a)), (ii) the down-to-top scheme [116], with the waveguide under the Ge photodetector (Figure 3(b)), and (iii) the side-coupled scheme [117], with tapered waveguide sitting in close proximity to the Ge photodetector (Figure 3(c)). The coupling loss hinges upon structural parameters of the waveguide and the Ge detector, wavelength, and polarization [37, 119, 120]. To facilitate a gradual light transfer, injection stages are tapered to wider or narrower waveguides, respectively. The butt-coupling approach, shown in Figure 3(d), is a tolerant and efficient injection scheme, typically yielding better optical absorption per device length as compared to evanescent-coupling schemes. Moreover, butt-coupling usually requires less design effort, as the detector and the waveguide are connected to each other on the same plane. Here, low-loss coupling is governed by the mode-matching between the Si waveguide and the Ge photodetector. Improved coupling essentially requires tapered input stages to match the width of the Ge layer, possibly with or without additional Ge [121] or poly-Si [122] overlayers.

Incorporating Ge seamlessly into Si circuits is highly desirable. Initial issues imposed by the baseline process, including thermal budget constraints, contamination, and device size, are mastered, nowadays [123–125]. Available standards and solutions have reached levels of maturity high enough to support various kinds of nanophotonics applications, enabling them to make a seamless transition from research laboratories toward industry. A modular approach is typically adopted to have a reliable Si-foundry flow with a maximum compatibility with CMOS processes. High-performance Ge photodetectors are fabricated using well-established front-end-of-line ion implantation and epitaxy processes. Metal contacts (for heaters, modulators and detectors) are fabricated using mature back-end-of-line CMOS metallization processes and schemes. A cross-sectional view of CEA LETI's Si photonic platform is shown in Figure 4(a). SEG in a CVD tool is used, after an "HF-Last" wet cleaning to selectively grow thanks to GeH_4 hundreds of nm thick Ge layers in cavities (butt-coupling) or in windows surrounded by dielectrics. Global and local loading effects (i.e. the vast growth rate increases, occurring when switching from fullsheet wafers to patterned wafers and, on the latter, from large and closely packed Si windows to small, isolated window), together with faceting are accounted for by reducing precursor mass-flows and growth durations, growing more than the desired thickness and using chemical mechanical polishing to get rid of the overflowing material and recover smooth Ge surfaces. A cross-sectional scanning electron microscopy (SEM) image of a waveguide-coupled Si–Ge photodetector with lateral p-i-n hetero-junctions is shown in Figure 4(b). A robust fabrication flow has been developed on 200 and 300 mm wafers [126, 127], with a large-scale integration of

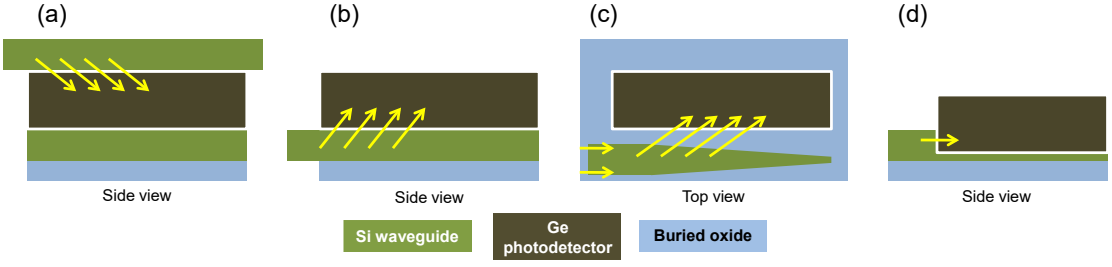

Figure 3: Waveguide-to-detector coupling configurations.
Evanescent-coupling schemes: (a) top-to-down, (b) down-to-top, and (c) side-coupling. (d) Butt-coupling scheme.

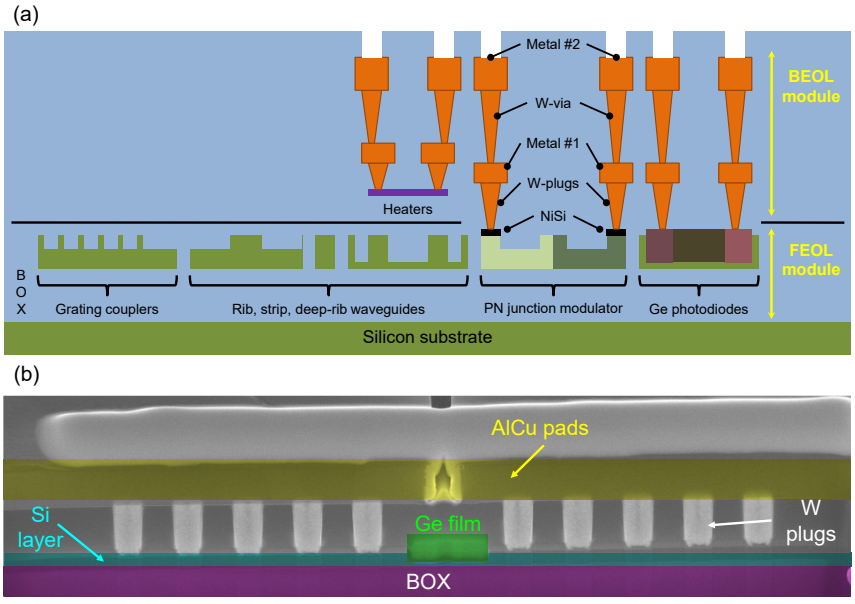

Figure 4: (a) Cross-sectional schematics of the full CEA LETI's silicon photonic platform for monolithic integration of passive and active chip components. (b) Scanning electron microscopy image of chip-integrated Si–Ge photodetector with a lateral p-i-n hetero-junction.

passive and active devices as open-access foundry models [19, 92, 128]. Si technology also continues to expand its frontiers towards radio-frequency and electronic circuitry. Photonic-electronic co-integration on the same substrate could yield full transmitters and receivers with subsidiary drivers, trans-impedance amplifier (TIA) and limiting amplifier (LA), thermal stabilizers and clock data recovery functions [129–132]. Ge-based photodetectors are also available on sub-micrometric [126, 127] and microns thick [133, 134] silicon-on-insulator (SOI) substrates, with high performances at mainstream communication wavelengths, i.e. 1.3 and 1.55 µm, typically.

4 Cutting-edge silicon–germanium photodetectors

The common types of Ge photodetectors integrated on Si waveguides are MSM or p-i-n devices. They are schematically shown in Figure 5. MSM photodetectors, shown in Figure 5(a), rely on interdigitated metal layers on top of Ge, with Schottky barriers. These devices have a simple structure, are easy to fabricate and have a low-bias operation [118, 121, 135–137]. Improved responsivities coupled with fast responses and high bit rates were shown over the years. However, MSM devices consistently exhibit very high dark currents due to the low Schottky barrier on Ge. High dark-current levels result in low signal-to-noise ratio, poor sensitivity and considerable power consumption [118, 135, 137]. Waveguide-integrated p-i-n's are the most attractive diode architectures.

4.1 P-i-n photodiodes

P-i-n photodiodes, in lateral (Figure 5(b)) or vertical (Figure 5(c)) configurations, consist in an intrinsic light-absorbing region sandwiched between highly doped *p*-type and *n*-type regions. So far, a large number of p-i-n diodes have been proposed and demonstrated in full-Ge (homojunctions – Figure 6(a)) [106, 138–141] and Si–Ge–Si (hetero-junctions – Figure 6(b)) [142–152] device arrangements. Single material detectors lack good light

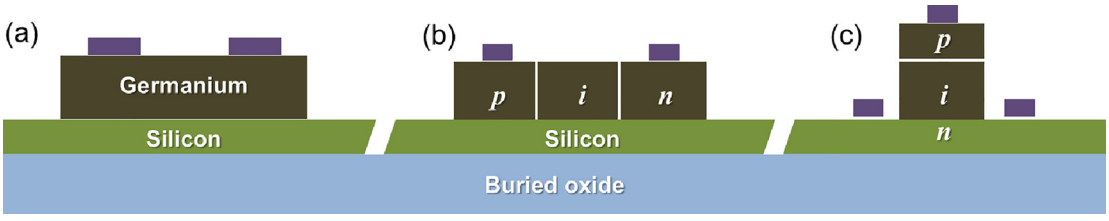

Figure 5: Common types of waveguide-integrated Si–Ge photodetectors.
(a) MSM structure, (b) lateral, and (c) vertical p-i-n diodes.

confinement due to the weak index contrast between intrinsic and doped regions. With such a device architecture, the optical mode (left-sided inset in Figure 6(a)) overlaps all Ge regions. This potentially results in the optical recombination of photo-generated carriers, which would otherwise contribute to the photocurrent, degrading the responsivity. In addition, homojunction p-i-n schemes require heavily doped Ge and metal via-plugs on Ge. This may cause a performance drop, yielding structures with lower responsivity, reduced speed, and higher noise. Moreover, ion implantation in and metal deposition on Ge are not as mature as in/on Si. Setting aside those shortcomings, homojunction devices can support bias-free operation at high transmission bit rates as the junction is without band gap energy discontinuities. The electric field inside the depletion region is high enough to extract the vast majority of generated photo-carriers at 0 V. As long as higher dark current, reduced responsivity, and slower response are addressed drawbacks, homojunction photodiodes may appear as an attractive choice for (use in) fast detection systems [106].

P-i-n photodiodes with Si–Ge–Si hetero-junctions were shown to be promising alternatives to homojunction devices. P-i-n hetero-junction diodes leverage all benefits of a full Si processing (doping by ion implantation and metal via-contacts fabrication occur directly in/on Si). The very same process steps can then be used to simultaneously dope and, later on in the overall process flow, electrically contact Si optical modulators and Si–Ge–Si photodetectors. This substantially simplifies the fabrication flow in Si foundries, lowering wafer-level production costs. Heavily doped *p*-type and *n*-type slabs are defined by masking and ion implantation in the Si layer. Deep cavities with a Si floor and Si sidewalls are etched then filled with selectively grown Ge, resulting in an intrinsic Ge absorption region in-between the *n*-type and *p*-type Si regions. From an optical point of view, the Si–Ge–Si hetero-junction diode arrangement yields a much better control over the modal confinement in the intrinsic region [150], as the excited modes stay confined within the intrinsic zone (right-sided inset of Figure 6(b)). This reduces the deleterious absorption losses of generated photo-carriers in the heavily doped regions. In opposition to full-Ge homojunction devices, the responsivity and bandwidth are low at 0 V for hetero-junction diodes [150–152]. Indeed, p-i-n devices rely on the presence of built-in electric field in the junction, which is not strong with such a heterostructure. Indeed, Si–Ge–Si devices have energy barriers at the Si–Ge interfaces that limit carrier collection at zero-bias. Typically, an additional reverse voltage of less than 0.5 V [150, 151] or 1 V [152] needs to be supplied to the device to enhance its collection efficiency. Present works on hetero-junction p-i-n diodes demonstrated a great potential for on-chip detection of high-speed signal traffics [145–152]. In particular, besides the first demonstration of a vertical hetero-junction diode by Ahn et al. [113], Zhang et al. reported a novel Si-contacted diode scheme, obtaining a

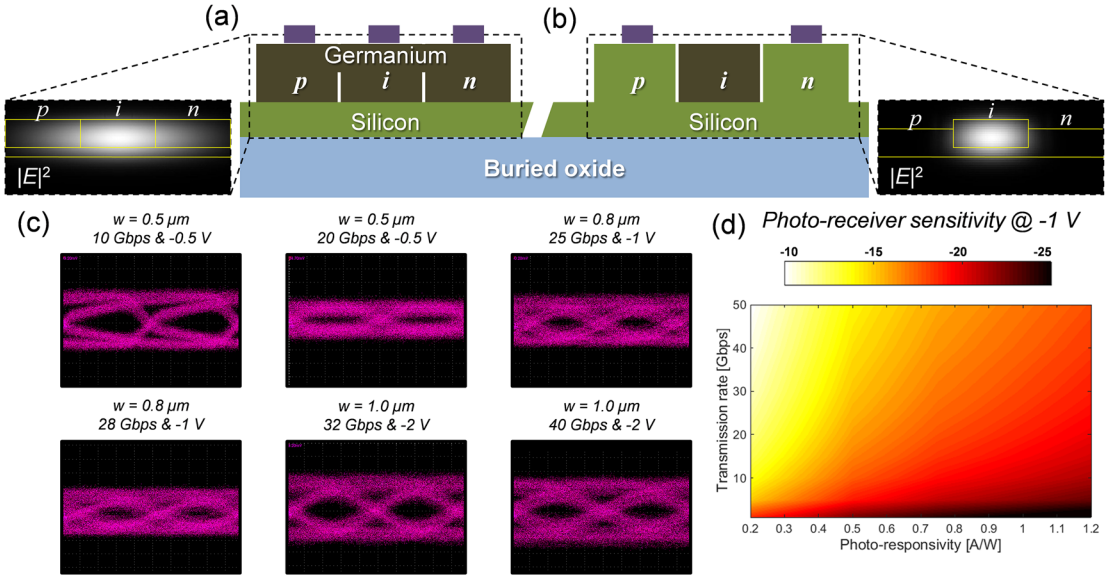

Figure 6: Lateral p-i-n photodetectors in (a) Ge homo-junction and (b) Si–Ge–Si hetero-junction configurations. Insets: Optical field profiles of the fundamental quasi-transverse electric modes in both types of structures. (c) Eye diagram apertures of various Si–Ge–Si p-i-n photodetectors with a lateral hetero-junction operated under low-biases and different bit rates. (d) Estimated receiver sensitivity with hetero-junction Si–Ge–Si photodetectors operated at –1 V, for a 1.55 μm wavelength and different transmission bit rates. The minimum detected power is defined at 10^{-12} BER, considering a TIA with an equivalent noise current density of 15 pA/Hz$^{1/2}$.

photo-responsivity of 1.14 A/W and a bandwidth of 20 GHz. However, the device was operated with a –4 V bias supply [145]. Chen et al. [147], in contrast, reported on a set of low-voltage-operated diodes that support a 28 Gbps detection at *C*-band wavelengths, with responsivities of 0.5 and 1 A/W for vertical and lateral layouts, respectively. Furthermore, the same group elaborated on an optimized lateral Si–Ge–Si p-i-n diode reversely biased at 1 V only. High responsivity–bandwidth products of ~50 and ~41 A/W-GHz were then obtained at 1.55 and 1.31 μm [122]. Such performances make those devices suitable for high-speed detection at bit rates of 56 Gbps and beyond [148, 149]. Benedikovic et al. [151] obtained 0.5-V-biased hetero-structured p-i-n devices with a close-to-limit responsivity of 1.2 A/W at 1.55 μm. Fast signal detections at conventional bit rates of 10, 20, and 25 Gbps were also achieved. Received power sensitivities, at a bit-error-rate (BER) of 10^{-9}, were in –14 dBm to –11 dBm range. Figure 6(c) shows eye diagrams of various hetero-structured p-i-n diodes operated at low voltages for different transmission bit rates. Compared to homojunction devices, another advantage of hetero-junction p-i-n photodiodes lies in their low dark current, typically in a 4 nA [122, 143, 147, 148] to 150 nA range [142, 145, 146, 149–152].

However, for the most part, p-i-n photodetectors yield insufficient electrical output levels. They thus rely on extra electronic stages attached to the chip [135]. The receiver input-referred noise is then dominant over the intrinsic photodetector noise, becoming one of the factors restricting the receiver sensitivity. Figure 6(d) shows the estimated sensitivity of a 1.55 μm photonic receiver based on hetero-structured p-i-n photodiodes, with parameters experimentally measured in Ref. [152]. Input-referred noise of TIA of 15 pA/Hz$^{1/2}$ and BER of 10^{-12} were considered in calculations [153]. The receiver sensitivity then degrades as the transmission speed increases, as the receiver noise increases with the bandwidth. The receiver sensitivity can be improved by increasing the photodetector responsivity. For regular "diode mode" operation at a single wavelength, i.e. operation regime without an internal multiplication gain, the photo-responsivity yield remains limited by the photon-to-electron conversion efficiency. A summary of the performances state-of-the-art Si–Ge photodetectors operated at low voltages is provided in Table 1.

4.2 Avalanche photodiodes

Avalanche photodetectors (APDs) are broadly used in optoelectronics and communications to detect low signal intensities. APDs rely on internal multiplication gain by exploiting an impact ionization effect as long as the electrical field is strong enough. Impact ionization enables generation of multiple photo-carriers, i.e. several electron–holes pairs are being generated per one absorbed photon,

Table 1: Summary of state-of-the-art waveguide-integrated Si–Ge photodetectors operating at standard communication wavelengths.

Reference	Type	λ [μm]	V_r (V)	I_d (A)	R_p (A/W)	f (GHz)	BR (Gbps)	P_{rec} (dBm)@BER
[118]	MSM	1.31	1.0	90 μ	0.42	35@2 V	40@1.5 V	–
		1.55			0.14			
[119]	V-p-i-n	1.55	1	1.6 n	1.0	40	–	–
[121]	MSM	1.55	1	100 n	0.40	40	–	–
[135]	MSM	1.31	1	120 μ	0.5	40	40	$-0.8@10^{-12}$
[138]	V-n-i-p	1.53	1	3 n	0.8	45	–	–
[139]	L-p-i-n	1.55	1	4 n	0.8	120	40@0 V	–
[140]	L-p-i-n	1.55	0.5	500 n	0.8	14–19	–	–
[106]	L-p-i-n	1.55	1	32 n	0.52–0.78	45–90	25/40	$-15.4/-14@10^{-12}$
[142]	V-p-i-n	1.55	1	160 n	0.75	17@4 V	–	–
[143]	V-p-i-n	1.55	1	7.7 n	0.75	31.7	–	–
[145]	L-p-i-n	1.55	4	120 n	1.14	20	40	–
[146]	L-p-i-n	1.55	1	100 n	1	70	–	–
[147]	V-p-i-n	1.55	1	11 n	0.4–0.6	50	28	–
	L-p-i-n			3.3 n	1.0	20		
[121]	L-p-i-n	1.31	1	2.5 n	0.98	50	50/56	–
		1.55			0.72	45	50/56	
[150]	L-p-i-n	1.55	1	207 n	1.1	5–37	–	–
[151]	L-p-i-n	1.55	1	100 n	1.2	7	10–25	-14 to $-11@10^{-9}$
[152]	L-p-i-n	1.55	1	100 n	0.17–1.16	7–35	10–40	–

MSM, metal–semiconductor–metal diode; V-p-i-n, vertical p-i-n diode; L-p-i-n, lateral p-i-n diode; λ, operating wavelength; V_r, reverse bias; I_d, dark current; R_p, photo-responsivity; f, cutoff frequency; BR, transmission bit rate; P_{rec}, received optical power; BER, bit-error-rate.

which in turn, enables to amplify the light signal. Consequently, multiplied photocurrents help to boost the signal-to-noise ratio and/or overcome the thermal noise of electrical amplifiers, improving the overall detection sensitivity. However, pure Ge detectors are noticeably noisy. The large intrinsic noise prevents them from being the first choice for use in aforementioned high-speed digital applications. As the Ge gap energy is low, electrons (α_e) and holes (β_h) have almost the same magnitude of ionization coefficients. Hence the carrier impact ionization ratio (k) is close to unity ($k = \beta_h/\alpha_e \approx 0.9$). By contrast, ionization coefficients of pure Si are asymmetric, yielding much lower impact ionization ratio ($k \approx 0.01$) [37–39]. It is worth to mention that similar to other APD parameters, the impact ionization ratio is also a function of the applied electric field. The k parameter is therefore a key figure of any APDs, as it directly relates to the avalanche excess noise, gain-bandwidth product, and device sensitivity – essential device- and system-level metrics.

Even though APDs have been studied since the 1960s and late 1970s [33, 34], it is only a decade ago that monolithically integrated Si–Ge APDs gathered research interest again thanks to works by Assefa et al. [137] and Kang et al. [154]. MSM, p-i-n, and separate absorption charge multiplication (SACM) structures are used in APDs [135, 144, 154–180]. SACM APDs advantageously combine the high absorption in Ge and the low multiplication noise of Si, yielding another degree of flexibility to engineer device performances. Most of the SACM structures use vertical diode architectures [154, 156, 159, 161–166, 174] instead of lateral ones [172, 176]. However, the vertical diode scheme calls upon more process steps, with dedicated epitaxy and metal contacting on Ge, which may degrade the overall performances. Moreover, typical SACM APDs use a single voltage to control electric fields in those, by design, separated regions [161–164]. This, in turn, calls upon delicate charge layer optimization, i.e. attentive tailoring of charge layer thickness, together with its doping profile. This, consequently, results in a fairly high design complexity. It is indeed crucial that the electric field is strong enough to trigger an impact ionization process in Si charge region. At the same time, the electric field has to remain below an ionization threshold in Ge, above which the tunneling dark current would substantially increase [31, 37].

Performant and reliable surface-illuminated and waveguide-coupled APDs have been reported at 10 Gbps bit rates with receiver sensitivities in the –18 to –28 dBm range, easily supporting single-channel transmission systems in the *O*- and *C*-wavebands [144, 154, 157–160]. MSM [137] and full-Ge p-i-n [156] are simpler to design and fabricate. They also operate at lower voltages. However, both type of devices suffer from high dark currents, jeopardizing future opto-electrical performance improvements. While noise is lower, the gain-bandwidth product is higher and, in general, performances are better with SACM devices [154–156, 159], they are driven with overly high voltages (>20 V) [154–156] that are comparable to bias levels needed for III–V-based devices [55–58]. Such excessively high voltage driving is not practical for many energy-aware applications, however [181] (Figure 7).

More recent works concentrated on APD structures, operating at low [160–166] or high [167, 168, 173–175] voltages, fitting the needs of on-off keying (OOK) systems with direct detection at 25 and 28 Gbps. More specifically, Chen et al. [160] demonstrated a 25 Gbps *O*-band receiver with vertical p-i-n APDs. A judicious thinning of the Ge layer in the intrinsic region down to 185 nm was leveraged to lower the driving voltage and suppress the avalanche multiplication noise through the dead space effect. This design also improved the gain-bandwidth product from 100 to 140 GHz and reduced the impact ionization ratio from 0.5 to 0.2 compared to the previous device layout [158]. The APD receiver was biased at sub-5 V only, yielding a sensitivity of –14.8 dBm for 10^{-9} BER. In addition, favored low-voltage operation (<10 V) at 25 Gbps was also demonstrated in two- and three-terminal SACM APDs [161, 162], both operated at 1.55 μm wavelength. Conventional full-receiver [161] and optimized receiver-less [162] devices had a similar gain-bandwidth product of about 280 GHz. Sensitivities reached –16 dBm (at BER of 10^{-12}) [161] and –11 dBm (at BER of 10^{-4}) [162] power levels, respectively.

Surging applications in chip-scale nanophotonics require devices able of detecting low signal intensities at speeds well-beyond 10 and 25 Gbps per single optical OOK carrier [6, 14]. For this, Kim et al. [169] proposed and demonstrated a receiver module with vertically illuminated Si–Ge APD. The device exploited a negative photoconductance effect for high-speed operation with high photo-gains. The gain-bandwidth product of a device reached a maximum of 460 GHz and clearly open eye patterns were reported for bit rates up to 50 Gbps. At a 10^{-12} BER threshold, device sensitivities varied from –19 to –14 dBm for 28 and 40 Gbps signals, respectively. However, reverse voltage in excess of 26 V impeded the practical use of such APD designs. In contrast, Benedikovic et al. [170] demonstrated a waveguide-integrated APD based on a simple p-i-n photodiode with lateral heterojunction operated at 1.55 μm telecom waveband. The Si–Ge–Si p-i-n APD benefits from a shrinked junction area and a localized impact ionization process taking place at the hereto-structured Si–Ge–Si interfaces. Si–Ge–Si APD with

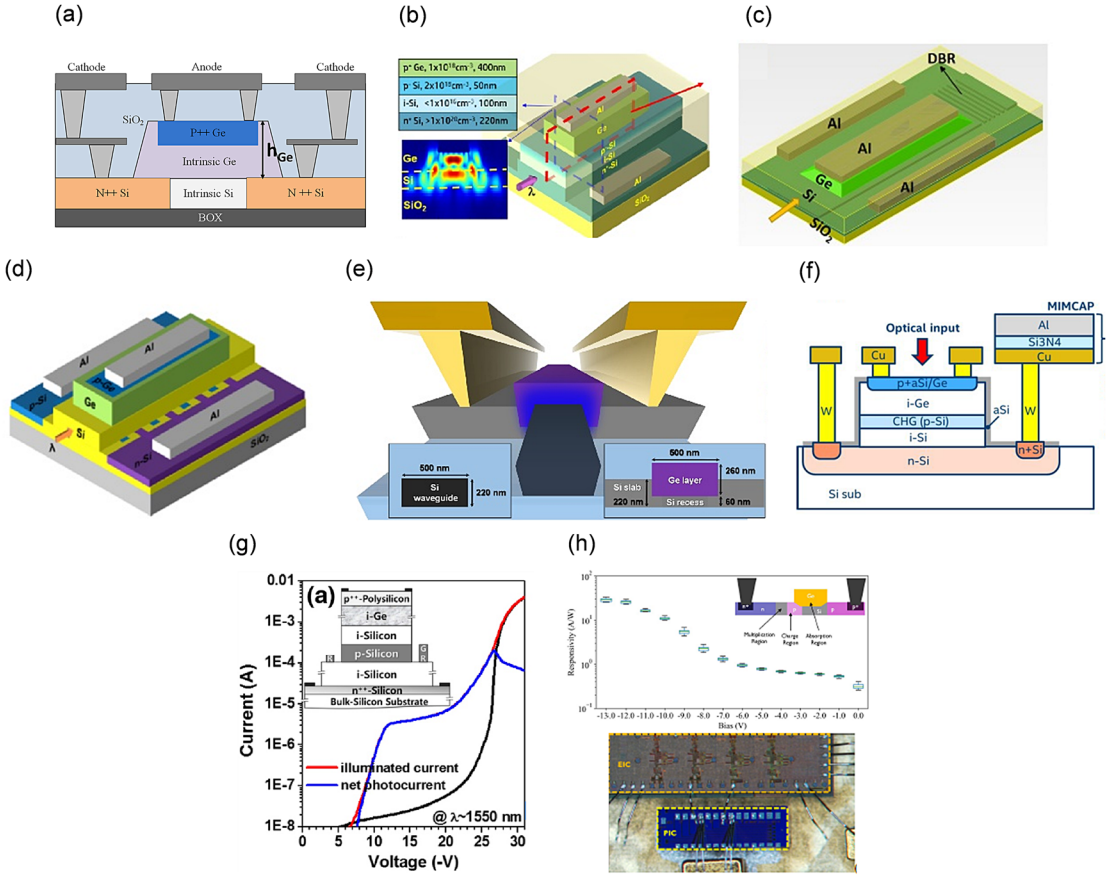

Figure 7: Photonic receivers made out of Si–Ge avalanche photodetectors.
(a) 28 Gbps vertical p-i-n APD. (b) 25 Gbps receiver based on two-stage vertical SACM APD. (c) 64 Gbps vertical SACM APD with DBRs. (d) 25 Gbps three-terminal vertical SACM APD. (e) 40 Gbps hetero-structured lateral p-i-n APD. (f) 50 Gbps receiver sub-system with a top-illuminated APD and an integrated metal–insulator–metal capacitor. (g) 40 Gbps receiver module with vertically illuminated APD. (h) 56 Gbps receiver with a waveguide-coupled lateral SACM APD. Figures adapted with permission from: (a) a study by Carpentier et al. [166]. (b) From a study by Huang et al. [161] © The Optical Society. (c) From a study by Wang et al. [163] © Chinese Laser Press. (d) From a study by Zeng et al. [162] © The Optical Society. (e) From a study by Benedikovic et al. [170] © The Optical Society. (f) From a study by Park et al. [171]. (g) From a study by Kim et al. [169] © The Optical Society. (h) From a study by Srinivasan et al. [172].

p-i-n hetero-structures yield simultaneous high-speed (gain-bandwidth product of 210 GHz) and low-noise operation (carrier impact ionization of ~0.25). Furthermore, an intrinsic photo-gain of 120 and a photo-responsivity of 59 A/W were generated for input power of –30 dBm only. 40 Gbps eye diagrams remained open for input powers down to –20 dBm, without using any electronic amplification stages. At a 10^{-9} BER and sub-10 V bias, lateral p-i-n APD sensed optical powers of –13 dBm for 32 Gbps and –11 dBm for 40 Gbps bit rates. In addition, Park et al. [171] have presented a 50 Gbps receiver sub-system operated at a more favorable sensitivity wavelength of 1.31 μm. The receiver comprised a top-illuminated APD and an integrated metal–insulator–metal capacitor. The measured receiver sensitivity was –16 dBm at 10^{-4} BER level. Another *O*-band photonic receiver has recently been demonstrated in a 55 nm SiGe BiCMOS technology by Srinivasan et al. [172, 176]. Receiver consisted then of a waveguide-coupled SACM APD [176], having a gain-bandwidth product of 300 GHz and supporting 56 Gbps signal detection with a sensitivity of –19 dBm (at 10^{-4} BER) and a power consumption of 140 mW [172]. Performance metrics of state-of-the-art Si–Ge avalanche photo-receivers are summed up in Table 2.

Improved capability of on-chip Si–Ge detectors has also been investigated using spectrally efficient multi-level formats such as 4-level pulse amplitude modulation (PAM-4) [163–165, 177–180] rather than conventional OOK modulation [137, 144, 154, 157–162, 164, 166, 169–173, 176]. Verbist et al. [177] obtained an APD with 40 Gbps and 50 Gbps PAM-4 detection through 42 and 10 km long transmission links. Wang et al. [178] successfully demonstrated another

50 Gbps PAM-4 transmission using a *C*-band two-terminal SACM APD [161], yielding 10^{-4} BER sensitivity of –17 dBm. Yuan et al. showed the superior temperature performance of a sub-10 V operated PAM-4 Si–Ge APD [182]. Clearly open eye diagrams at 64 Gbps were retrieved for temperatures in the 30–90 °C range. However, power sensitivity was not quantified here. Huang et al. [163, 180] demonstrated a low-voltage Si–Ge APD with distributed Bragg reflectors (DBRs). Indeed, optimized DBRs reflect the unabsorbed light back to the SACM APD, which in turn, substantially enhances the device quantum efficiency from 60 to 90%. DBR-assisted APDs also favor a high-speed operation with an impressive gain-bandwidth product of 500 GHz, facilitating a detection up to 64 Gbps for PAM-4 modulated signals. Power sensitivity of –13 dBm at 10^{-4} BER and –4 dBm at 10^{-12} BER were demonstrated [163].

Si–Ge APDs can also be advantageously exploited in emerging fields such as photon counting, quantum key distribution or single-photon detection [182, 183], imaging [184], or light detection and ranging [185], to name a few. Indeed, single-photon Si–Ge APDs can be used in mainstream fiber communication windows, which is not the case of more mature Si alternatives [186, 187]. Meanwhile, state-of-the-art single-photon APDs at NIR wavelengths are mostly III–V structures, which are still more costly and difficult to integrate with Si CMOS processes [188].

4.3 High-power photodiodes

The research and development of low-power detectors, for applications mainly in optoelectronics and communications, have been key enabler in advances behind high-speed transmissions of our digital society. There is, however, a rising interest in devices relying on microwave systems and analog links [189, 190], both leveraging the reliability and cost-effectiveness of nanophotonic platforms. Optical photodetectors capable of handling high-power levels are essential in such links [191–193]. To improve the power-handling capacity of waveguide-integrated Si–Ge photodetectors, a few promising solutions have been reported in recent years [119, 194–198]. A limitation with low-power detector designs is that they mostly rely on a waveguide-coupled chip architecture with evanescent or butt-coupling light injection. With such designs, the waveguide light is injected into the photodetector through a Si–Ge junction, producing multi-modal interferences with rather high peak intensities. Light absorption mainly occurs in the front part of such devices, i.e. the one close to the Si–Ge junction. Both effects are typically negligible, if photodetector is operated at lower power levels. They, however, become issues at higher input powers, resulting in undesired power saturation (Figure 8).

Byrd et al. [119] designed a mode-evolution-based coupler to feed Si–Ge photodetectors. Indeed, a tapered coupler favors uniform light transfer from the waveguide to the detector, reducing current saturation at high-power levels thanks to carrier screening effect. Under high-power illumination, a side-coupled approach yielded better photocurrent generation up to ~16 mA and a 40-fold bandwidth enhancement compared to butt-coupled schemes. Such a Si–Ge detector provides high responsivity (1 A/W), low dark current (1.16 nA), and 40-GHz bandwidth. Li et al. [194] investigated high-power characteristics of a normal-incidence n-i-p-i-n back-to-back dual-absorption photodetector. They obtained a saturated photocurrent up to ~21 mA at low voltages, with a 4 GHz cutoff frequency and responsivities of 0.31 and 0.52 A/W at 1.55 and 1.31 µm wavelengths. Integrated high-power Si–Ge photodetectors assisted by light field

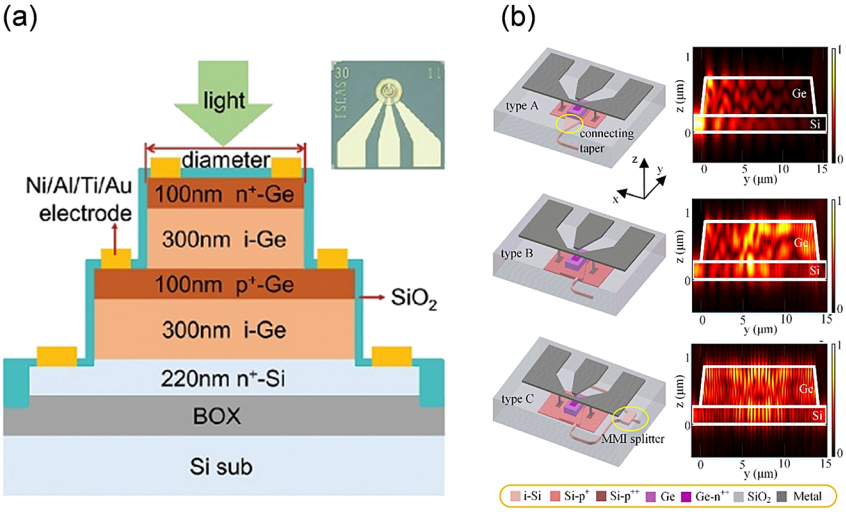

Figure 8: High-power Si–Ge photodetectors. (a) Back-to-back top-illuminated dual-absorption photodiode. (b) Photodetector based on a light field manipulation. Figures adapted with permission from: (a) a study by Li et al. [194] © The Optical Society. (b) From a study by Zuo et al. [195] © The Optical Society.

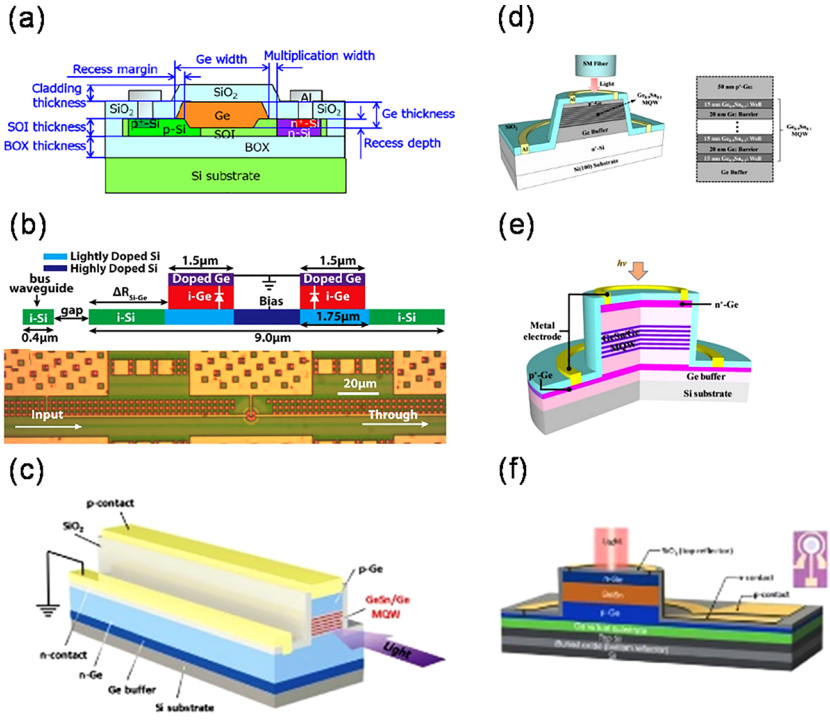

Figure 9: Si–Ge photodetectors for extended spectral operation.
(a) Waveguide-coupled APD with a lateral SACM region. (b) Whispering gallery p-i-n resonant photodetector. (c) P-i-n photodetector with strained GeSn/Ge MQWs. (d) $Ge_{0.9}Sn_{0.1}$ MQW p-i-n photodiode on Si substrate. (e) GeSn/Ge MQW p-i-n photodiode on 300 mm Si substrate (f) Resonant-cavity-enhanced GeSn photodetector. Figures adapted with permissions from: (a) a study by Ono et al. [202]. (b) From a study by Su et al. [203] © The Optical Society. (c) From a study by Huang et al. [204] © The Optical Society. (d) From a study by Dong et al. [205] © The Optical Society. (e) From a study by Xu et al. [206] © The Optical Society. (f) From a study by Tsai et al. [207] © The Optical Society.

manipulation were fabricated by Zuo et al. [195]. The inhomogeneous light distribution in the absorber was addressed thanks to a multimode waveguide with a taper structure, resulting in a better absorption profile. Under high-power injection, saturation photocurrent up to ~27 mA was generated. High-power and high-speed operation was achieved at 10 Gbps data rate in a 5–11 mA power range. Chang et al. [196] introduced a four-stage dual-fed distributed traveling-wave photodetector that boosted the power-handling capability. A maximum DC photocurrent of 112 mA and a 3-dB bandwidth up to 40 GHz were demonstrated, together with opened eye diagrams for 10 and 40 Gbps signals. A similar concept, with a 16-stage distributed traveling-wave photodetector was investigated by Bogaert et al. [197], achieving DC photocurrent of about 100 mA and a bandwidth of 27.5 GHz. An improved distributed traveling-wave photodetector design was reported by Fu et al. [198] with the help of an aperiodically loaded open-circuit electrode. This configuration yielded maximum output powers of 10.2 and 6.5 dBm at 5 and 10 GHz cutoff frequencies, respectively.

4.4 Photodiodes beyond mainstream wavebands

Exploring new wavebands for optoelectronics and communications, beyond standardized datacom and telecom regions, opens up new arenas in chemical, biological and medical sensing, imaging and monitoring. Combining (i) group-IV nanophotonics and Si-foundry-compatible processing and (ii) low-loss hollow-core fibers and wideband thulium-doped fiber amplifiers at 2-μm is promising for next-generation on-chip systems [199–201]. Advanced strategies have to be conducted for high-performance photodetectors in these areas, as the operation of conventional Si–Ge devices is limited by the Ge cut-off wavelength around 1.6 μm (Figure 9).

Extended operation of Si–Ge photodetectors in the *L*-band and *U*-band wavelengths (1.565–1.625 μm and 1.625–1.675 μm) has been successfully demonstrated by several groups [202–204, 208–210]. This mainly includes approaches with Ge MSM detectors with recessed silicon nitride sidewall stressor [208], lateral waveguide-coupled SACM APDs with low polarization dependence [202], structures combining avalanche multiplication and enhanced Franz–Keldysh effect [209, 210], whispering gallery photodetectors [203] or devices with multiple-quantum-well (MQW) active layers [204]. Improved light detection at longer wavelengths has been achieved by Anthony et al. [211] by harnessing indirect band transitions in pure Ge. Prototype 50 μm long p-i-n diodes and 14 μm long SACM APDs operated in the 1.85–2 μm spectral window yielded responsivities of 20 to 5 mA/W and 0.31 to 0.08 A/W, respectively. Defect-mediated photodetection at 2 μm was demonstrated by Zhao et al. [212] using a 500 μm

Table 2: Properties of state-of-the-art Si–Ge avalanche photo-receivers operated at conventional optical communications wavebands.

Reference	λ (μm)	Modulation	V_{br} (V)	GBP (GHz)	k	BR (Gbps)	P_{rec} (dBm)@BER
[137]	1.31/1.5	OOK	3.5	300	0.20	10	$-13.9@10^{-9}$
[144]	1.3	OOK	20	115	–	25	$-30.5@10^{-10}$
[154]	1.3	OOK	25	340	0.09	10	$-28@10^{-12}$
[155]							
[156]	1.55	–	29.4	310	–	–	–
[157]	1.55	OOK	7	190	0.4	10	$-26@10^{-7}$
[158]	1.55	OOK	6.2	100	0.5	10	$-24.4@10^{-9}$
[159]	1.55	OOK	31	432	–	10	$-18.3@10^{-12}$
[160]	1.31	OOK	5	140	0.2	25	$-14.8@10^{-9}$
[161]	1.55	OOK	10	276	0.05	25	$-16@10^{-12}$
[162]	1.55	OOK	6	280	–	25	$-11.4@10^{-4}$
[163]	1.55	PAM-4	10	500	–	64	$-13@10^{-4}$
[164]	1.55	PAM-4	10	280	–	50	$-16@10^{-4}$
[165]	1.31	PAM-4	>15	–	–	112	$-8@10^{-4}$
[166]	1.55	OOK	6	400	–	28	$-9@10^{-12}$
[167]	1.31	OOK	>20	240	–	25	$-22.5@10^{-12}$
[168]	1.31	–	>18	101	–	–	–
[169]	1.31/1.55	OOK	>30	460	–	40	$-13.9@10^{-12}$
[170]	1.55	OOK	11	210	0.25	40	$-11.2@10^{-9}$
[171]	1.31	OOK	12	150	–	50	$-16@10^{-4}$
[172]	1.31	OOK	13	300	–	56	$-18.6@10^{-4}$

λ, wavelength; OOK, on-off keying modulation format; PAM-4, four-level pulse amplitude modulation format; V_{br}, breakdown voltage; GBP, gain-bandwidth product; k, carrier impact ionization ratio; BR, transmission bit rate; P_{rec}, received optical power; BER, bit-error-rate.

long Ge-based p-i-n detector, reaching a responsivity up to 0.25 A/W at 5 V reverse bias.

Most recently, germanium-tin (GeSn) layers on Si–Ge attracted considerable research attention to facilitate reliable on-chip photodetection well-over the *L*-waveband. Sn is, indeed, a semimetal, with therefore a 0 eV band gap, while the direct bandgap of Ge is 0.8 eV. Alloying the two of them pushes the photodetection wavelengths to values much higher than 1.6 μm as for pure Ge [54, 199]. A tunable direct bandgap can otherwise be obtained for a Sn content 8% and above in unstrained layers, for higher Sn contents in compressively strained layers, improving control over the photodetection wavelength range. Research on GeSn photodetectors progresses steadily toward low dark-current devices, with improved photo-responsivity, faster responses and even longer spectral reaches. However, those characteristics are rather difficult to meet simultaneously within a single device. Most mature GeSn photodetector designs include simple p-i-n diodes in the waveguide-integrated [210, 213] and free-space forms [214], MQW p-i-n photodiodes on Si [205, 206, 215] or Ge-on-insulator [216, 217] substrates, p-n-p floating-based hetero-junction phototransistors [218, 219], pseudomorphic hetero-junction p-i-n diode with resonant cavity [207], and MQW APDs [220, 221]. The opto-electrical performances of wavelength-extended Si–Ge photodetectors realizations still do not reach the same levels of Ge devices operating at standard fiber-optic telecommunication windows. Much more research efforts are still required.

5 Conclusions

In summary, we have reviewed recent advances in the field of Si–Ge photodetectors for applications in optoelectronics and communications at commercially harnessed NIR and SWIR wavelength ranges (1.31 and 1.55 μm). Si–Ge photodetectors are developing at a remarkable pace on a year-by-year basis, owing to breakthroughs in material processing, CMOS integration and device designs and engineering. A great advantage of Si–Ge photodetectors over existing alternatives (III–V-based devices, mainly) lies in the well-mastered and modern chip manufacturing in a Si environment and its perspective of compatibility with electronic circuits integration. This includes a wide variation of affordable SOI platforms, high-quality Ge epitaxy, cost-sharing Si foundry models, and broadened opportunities for photonic-electronic co-integration. Si and Ge complement each other thanks to their favorable electrical and optical properties and great process compatibility. This, in turn, favors the fabrication of sensitive photo-receivers that can be fast, less-noisy and energy-efficient. Indeed, Si and Ge also form a versatile nanophotonic platform, where the function of photodetection can be integrated

monolithically on the same chip, alongside with equally important functions such as lasing, high-speed light modulation and low-loss light routing and manipulation. For many kinds of p-i-n and avalanche Si–Ge detectors operating at standardized communication wavelengths, device performances are superior or at least on par with existing III–V devices. Researches aiming at improving the detection speed, reducing the bias supply, and reaching even lower detected power levels are on-going. Proving the full potential of Si–Ge photo-receivers not only as individual network elements, but especially as a part of all-optical communication line on a chip within target applications is another challenge. Rising applications in analog and microwave nanophotonics, as well as new areas at longer spectral wavebands otherwise call upon advanced photodetector concepts. Available solutions are less mature nowadays compared to their established datacom and telecom counterparts. High-power photodetectors still call upon specific electro-optical designs and typically suffer from lower fabrication tolerance. In addition, even though improvements in dark currents, responsivity, bandwidth and even longer spectral reach were achieved in GeSn photodetectors, required performance metrics are rarely obtained on single devices. Designs, fabrication and production schemes are hurdles to be overcome. As the interest in group-IV-based photodetectors continues to evolve, prospects remain bright and emerging challenges are going to be solved. Most likely, exciting research times and market opportunities will open up in front of Si–Ge photodetectors.

Acknowledgement: This work was funded by the European Research Council (ERC) under the European Union's Horizon 2020 Research and Innovation Program (ERC POPSTAR - grant agreement 647342). This work was also supported by Technological Research Institute (IRT) Nanoelectronics Nano 2022 and Important Project of Common European interest (IPCEI).

Author contributions: All the authors have accepted responsibility for the entire content of this submitted manuscript and approved submission.

Research funding: This work was funded by the European Research Council (ERC) under the European Union's Horizon 2020 Research and Innovation Program (ERC POPSTAR – grant agreement 647342). This work was also supported by Technological Research Institute (IRT) Nanoelectronics Nano 2022 and Important Project of Common European interest (IPCEI).

Conflict of interest statement: The authors declare no conflicts of interest regarding this article.

References

[1] L. Atzori, A. Iera, and G. Morabito, "The Internet of things: survey," *Comput. Netw.*, vol. 54, no. 15, pp. 2787–2805, 2010.

[2] I. Demirkol, D. Camps-Mur, J. Paradells, M. Combalia, W. Popoola, and H. Haas, "Powering the Internet of things through light communication," *IEEE Commun. Mag.*, vol. 57, no. 6, pp. 107–113, 2019.

[3] R. Sabella, "Silicon photonics for 5G and future networks," *IEEE J. Sel. Top. Quantum Electron.*, vol. 26, no. 2, p. 8301611, 2020.

[4] C. Doerr and L. Chen, "Silicon photonics in optical coherent systems," *Proc. IEEE*, vol. 106, no. 12, pp. 2291–2301, 2018.

[5] M. Filer, J. Gaudette, Y. Yin, D. Billor, Z. Bakhtiari, and J. L. Cox, "Low-margin optical networking at cloud scale," *J. Opt. Commun. Netw.*, vol. 11, no. 10, pp. C94–C105, 2019.

[6] D. Liang, G. Kurczveil, Z. Huang, et al., "Integrated green DWDM photonics for next-gen high-performance computing," in *Optical Fiber Communication Conference*, Optical Society of America, 2020, p. Th1E.2.

[7] Q. Cheng, M. Bahadori, M. Glick, S. Rumley, and K. Bergman, "Recent advances in optical technologies for data centers: a review," *Optica*, vol. 5, no. 11, pp. 1354–1370, 2018.

[8] A. Alduino and M. Paniccia, "Wiring electronics with light," *Nat. Photonics*, vol. 1, no. 3, pp. 153–155, 2007.

[9] R. G. Beausoleil, P. J. Kuekes, G. S. Snider, S.-Y. Wang, and R. S. Williams, "Nanoelectronic and nanophotonic interconnect," *Proc. IEEE*, vol. 96, no. 2, pp. 230–247, 2008.

[10] D. A. B. Miller, "Saving energy and increasing density in information processing using photonics," in *Optical Fiber Communication Conference*, Optical Society of America, 2020, p. Th1E.1.

[11] The Institute of Electrical and Electronics Engineers. IEEE P802.3ba, 40 Gb/s and 100 Gb/s ethernet task force, 2010. Available at: http://www.ieee802.org/3/ba/.

[12] The Institute of Electrical and Electronics Engineers. IEEE P802.3bs, 200 Gb/s and 400 Gb/s ethernet task force, 2018. Available at: http://www.ieee802.org/3/bs/.

[13] 2018 ethernet alliance roadmap. Available at: http://www.ethernetalliance.com.

[14] E. Timurdogan, Z. Su, R.-J. Shiue, et al., "400G silicon photonics integrated circuit transceiver chipsets for CPO, OBO, and pluggable modules," in *Optical Fiber Communication Conference*, Optical Society of America, 2020, p. T3H.2.

[15] Semiconductors: the humble mineral that transformed the world. Available at: http://www.bbc.com/future/bespoke/made-on-earth/how-the-chip-changed-everything/.

[16] C. Sun, M. T. Wade, Y. Lee, et al., "Single-chip microprocessor that communicates directly using light," *Nature*, vol. 528, no. 7583, pp. 534–538, 2015.

[17] A. H. Atabaki, S. Moazeni, F. Pavanello, et al., "Integrating photonics with silicon nanoelectronics for next generation of systems on a chip," *Nature*, vol. 556, no. 7701, pp. 349–354, 2018.

[18] A. Rahim, T. Spuesens, R. Baets, and W. Bogaerts, *Proc. IEEE*, vol. 106, no. 12, pp. 2313–2330, 2018.

[19] D. Thomson, A. Zilkie, J. E. Bowers, et al., "Roadmap on silicon photonics," *J. Opt.*, vol. 18, no. 7, p. 073003, 2016.

[20] D. Marris-Morini, V. Vakarin, J. M. Ramirez, et al., "Germanium-based integrated photonics from near- to mid-infrared

applications," *Nanophotonics*, vol. 7, no. 11, pp. 1781–1793, 2018.
[21] D. Patterson, I. De Sousa, and L.-M. Achard, "The future of packaging with silicon photonics," *Chip Scale Rev.*, vol. 17, no. 1, pp. 14–25, 2017.
[22] J. Cardenas, C. B. Poitras, J. T. Robinson, K. Preston, L. Chen, and M. Lipson, "Low loss etchless silicon photonic waveguides," *Opt. Express*, vol. 17, no. 6, pp. 4752–4757, 2009.
[23] R. Halir, A. Ortega-Moñux, D. Benedikovic, et al., "Subwavelength-grating metamaterial structures for silicon photonic devices," *Proc. IEEE*, vol. 106, no. 12, pp. 2144–2157, 2018.
[24] H. Rong, R. Jones, A. Liu, et al., "A continuous-wave Raman silicon laser," *Nature*, vol. 433, no. 7027, pp. 725–728, 2005.
[25] Y. Takahashi, Y. Inui, M. Chihara, T. Asano, R. Terawaki, and S. Noda, "A micrometre-scale Raman silicon laser with a microwatt threshold," *Nature*, vol. 498, no. 7455, pp. 470–474, 2013.
[26] N. T. Otterstrom, R. O. Behunin, E. A. Kittlaus, Z. Wang, and P. T. Rakich, "A silicon Brillouin laser," *Science*, vol. 360, no. 6393, pp. 1113–1116, 2018.
[27] F. T. Armand Pilon, A. Lyasota, Y.-M. Niquet, et al., "Lasing in strained germanium microbridges," *Nat. Commun.*, vol. 10, p. 2724, 2019.
[28] E. M. T. Fadaly, A. Dijkstra, J. R. Suckert, et al., "Direct-bandgap emission from hexagonal Ge and SiGe alloys," *Nature*, vol. 580, no. 7802, pp. 205–2019, 2020.
[29] G. T. Reed, G. Mashanovich, F. Y. Gardes, and D. J. Thomson, "Silicon optical modulators," *Nat. Photonics*, vol. 4, no. 8, pp. 518–526, 2010.
[30] M. Berciano, G. Marcaud, P. Damas, et al., "Fast linear electro-optic effect in a centrosymmetric semiconductor," *Commun. Phys.*, vol. 1, p. 64, 2018.
[31] J. Michel, J. Liu, and L. C. Kimerling, "High-performance Ge-on-Si photodetectors," *Nat. Photonics*, vol. 4, no. 8, pp. 527–534, 2010.
[32] P. C. Eng, S. Song, and B. Ping, "State-of-the-art photodetectors for optoelectronic integration at telecommunication wavelength," *Nanophotonics*, vol. 4, no. 3, pp. 277–301, 2015.
[33] Ch. L. Tan and H. Mohseni, "Emerging technologies for high performance infrared detectors," *Nanophotonics*, vol. 7, no. 1, pp. 169–197, 2017.
[34] J. N. Shive, "The properties of germanium phototransistors," *J. Opt. Soc. Am.*, vol. 43, no. 4, pp. 239–244, 1953.
[35] H. Melchior and W.T. Lynch, "Signal and noise response of high speed germanium avalanche photodiodes," *IEEE Trans. Electron Devices*, vol. 13, no. 12, pp. 829–838, 1966.
[36] T. Kaneda, H. Fukuda, T. Mikawa, Y. Banba, and Y. Toyama, "Shallow-junction p+-n germanium avalanche photodiodes (APD's)," *Appl. Phys. Lett.*, vol. 34, no. 12, pp. 866–568, 1979.
[37] L. Vivien and L. Pavesi, *Handbook of Silicon Photonics*, Boca Raton, CRC Press, 2013.
[38] L. Virot, "Développement de photodiodes à avalanche en Ge sur Si pour la détection faible signal et grande vitesse," Doctoral thesis, 2014. Available at: https://tel.archives-ouvertes.fr/tel-01136096.
[39] S. M. Sze and K. K. Ng, *Physics of Semiconductor Devices*, Hoboken, New Jersey, Wiley, 2006.
[40] Y. Gao, H. Cansizoglu, K. G. Polat, et al., "Photon-trapping microstructures enable high-speed high-efficiency silicon photodiodes," *Nat. Photonics*, vol. 11, no. 5, pp. 301–308, 2017.
[41] D. O. Caplan, "Laser communication transmitter and receiver design," *J. Opt. Fiber Commun. Rep.*, vol. 4, pp. 225–362, 2007.
[42] J. J. Ackert, D. J. Thomson, L. Shen, et al., "High-speed detection at two micrometres with monolithic silicon photodiodes," *Nat. Photonics*, vol. 9, no. 6, pp. 393–396, 2015.
[43] H. Cansizoglu, A. S. Mayet, S. Ghandiparsi, et al., "Dramatically enhanced efficiency in ultra-fast silicon MSM photodiodes via light trapping structures," *IEEE Photonics Technol. Lett.*, vol. 31, no. 20, pp. 1619–1622, 2019.
[44] J. J. Ackert, M. Fiorentino, D. F. Logan, R. Beausoleil, P. E. Jessop, and A. P. Knights, "Silicon-on-insulator microring resonator defect-based photodetector with 3.5-GHz bandwidth," *J. Nanophotonics*, vol. 5, no. 1, p. 059507, 2011.
[45] T. Tanabe, H. Sumikura, H. Taniyama, A. Shinya, and M. Notomi, "All-silicon sub-Gb/s telecom detector with low dark current and high quantum efficiency on chip," *Appl. Phys. Lett.*, vol. 96, no. 10, p. 101103, 2010.
[46] K. Preston, Y. H. D. Lee, M. Zhang, and M. Lipson, "Waveguide-integrated telecom-wavelength photodiode in deposited silicon," *Opt. Lett.*, vol. 36, no. 1, pp. 52–54, 2011.
[47] B. Desiatov, I. Goykhman, J. Shappir, and U. Levy, "Defect-assisted sub-bandgap avalanche photodetection in interleaved carrier-depletion silicon waveguide for telecom band," *Appl. Phys. Lett.*, vol. 104, no. 9, p. 091105, 2014.
[48] S. Wirths, R. Geiger, N. von den Driesch, et al., "Lasing in direct-bandgap GeSn alloy grown on Si," *Nat. Photonics*, vol. 9, no. 2, pp. 88–92, 2015.
[49] Q. Liu, J. M. Ramirez, V. Vakarin, et al., "On-chip Bragg grating waveguides and Fabry-Perot resonators for long-wave infrared operation up to 8.4 μm," *Opt. Express*, vol. 26, no. 26, pp. 34366–34372, 2018.
[50] T. Li, M. Nedeljkovic, N. Hattasan, et al., "Ge-on-Si modulators operating at mid-infrared wavelengths up to 8 μm," *Photon. Res.*, vol. 7, no. 8, pp. 828–836, 2019.
[51] J. M. Hartmann, A. Abbadie, A. M. Papon, et al., "Reduced pressure–chemical vapor deposition of Ge thick layers on Si(001) for 1.3–1.55-μm photodetection," *J. Appl. Phys.*, vol. 95, no. 10, pp. 5905–5913, 2004.
[52] C. G. Littlejohns, M. Nedeljkovic, C. F. Mallinson, et al., "Next generation device grade silicon-germanium on insulator," *Sci. Rep.*, vol. 5, p. 8288, 2015.
[53] C. G. Littlejohns, T. Dominguez Bucio, M. Nedeljkovic, et al., "Towards a fully functional integrated photonic-electronic platform via a single SiGe growth step," *Sci. Rep.*, vol. 6, p. 19425, 2016.
[54] R. Soref, "Silicon-based silicon–germanium–tin heterostructure photonics," *Philos. T. R. Soc. A*, vol. 372, no. 2012, p. 20130113, 2014.
[55] M. Cooke, "Silicon photonics and III-V integration," http://www.semiconductor-today.com/. Technical focus: III-Vs on silicon – Optoelectronics, vol. 11, no. 7, pp. 80–85, 2016.
[56] M. Nada, Y. Yamada, and H. Matsuzaki, "Responsivity-bandwidth limit of avalanche photodiodes: toward future ethernet systems," *IEEE J. Sel. Top. Quantum Electron.*, vol. 24, no. 2, p. 3800811, 2018.
[57] M. Nada, F. Nakajima, T. Yoshimatsu, et al., "High-speed III-V based avalanche photodiodes for optical communications—the forefront and expanding applications," *Appl. Phys. Lett.*, vol. 116, no. 14, p. 140502, 2020.

[58] Y. Yuan, D. Jung, K. Sun, et al., "III-V on silicon avalanche photodiodes by heteroexpitaxy," *Opt. Lett.*, vol. 44, no. 14, pp. 3538–3541, 2019.
[59] T. Komljenovic, D. Huang, P. Pintus, M. A. Tran, M. L. Davenport, and J. E. Bowers, "Photonic integrated circuits using heterogeneous integration on silicon," *Proc. IEEE*, vol. 106, no. 12, pp. 2246–2257, 2018.
[60] M. Takenaka, Y. Kim, J. Han, et al., "Heterogeneous CMOS photonics based on SiGe/Ge and III–V semiconductors integrated on Si platform," *IEEE J. Sel. Top. Quantum Electron.*, vol. 23, no. 3, p. 8200713, 2017.
[61] J. M. Ramirez, H. Elfaiki, T. Verolet, et al., "III-V-on-silicon integration: from hybrid devices to heterogeneous photonic integrated circuits," *IEEE J. Sel. Top. Quantum Electron.*, vol. 26, no. 2, p. 6100213, 2020.
[62] J. Zhang, A. De Groote, A. Abbasi, et al., "Silicon photonics fiber-to-the-home transceiver array based on transfer-printing-based integration of III-V photodetectors," *Opt. Express*, vol. 25, no. 13, pp. 14290–14299, 2017.
[63] B. Tossoun, G. Kerczveil, C. Zhang, et al., "Indium arsenide quantum dot waveguide photodiodes heterogeneously integrated on silicon," *Optica*, vol. 6, no. 10, pp. 1277–1281, 2019.
[64] I. Goykhman, U. Sassi, B. Desiatov, et al., "On-chip integrated, silicon–graphene plasmonic Schottky photodetector with high responsivity and avalanche photogain," *Nano Lett.*, vol. 16, no. 5, pp. 3005–3013, 2016.
[65] J. Gosciniak, F. B. Atar, B. Corbett, and M. Rasras, "CMOS-compatible titanium nitride for on-chip plasmonic Schottky photodetectors," *ACS Omega*, vol. 4, no. 17, pp. 17223–17229, 2019.
[66] J.-A. Huang and L.-B. Luo, "Low-dimensional plasmonic photodetectors: recent progress and future opportunities," *Adv. Opt. Mater.*, vol. 7, no. 13, p. 1900884, 2018.
[67] Y. Salamin, P. Ma, B. Baeuerle, et al., "100 GHz plasmonic photodetector," *ACS Photonics*, vol. 8, no. 5, pp. 3291–3297, 2018.
[68] J. Gosciniak and M. Rasras, "High-bandwidth and high-responsivity waveguide-integrated plasmonic germanium photodetector," *J. Opt. Soc. Am. B*, vol. 36, no. 9, pp. 2481–2491, 2019.
[69] P. Ma, Y. Salamin, B. Baeuerle, et al., "Plasmonically enhanced graphene photodetector featuring 100 Gbit/s data reception, high responsivity, and compact size," *ACS Photonics*, vol. 6, no. 1, pp. 154–161, 2019.
[70] K. Kim, J.-Y. Choi, T. Kim, S.-H. Cho, and H.-J. Chung, "A role for graphene in silicon-based semiconductor devices," *Nature*, vol. 479, no. 7373, pp. 338–344, 2011.
[71] F. H. L. Koppens, T. Mueller, P. Avouris, A. C. Ferrari, M. S. Vitiello, and M. Polini, "Photodetectors based on graphene, other two-dimensional materials and hybrid systems," *Nat. Nanotechnol.*, vol. 9, no. 10, pp. 780–793, 2014.
[72] D. Akinwande, C. Huyghebaert, C.-H. Wang, et al., "Graphene and two-dimensional materials for silicon technology," *Nature*, vol. 573, no. 7775, pp. 507–518, 2019.
[73] M. Romagnoli, V. Sorianello, M. Midrio, et al., "Graphene-based integrated photonics for next-generation datacom and telecom," *Nat. Rev. Mater.*, vol. 3, no. 10, pp. 392–414, 2018.
[74] S. Manzeli, D. Ovchinnikov, D. Pasquier, O. V. Yazyev, and A. Kis, "2D transition metal dichalcogenides," *Nat. Rev. Mater.*, vol. 2, no. 6, p. 17033, 2017.
[75] Y.-Q. Bie, G. Grosso, M. Heuck, et al., "A $MoTe_2$-based light-emitting diode and photodetector for silicon photonic integrated circuits," *Nat. Nanotechnol.*, vol. 12, no. 12, pp. 1124–1129, 2017.
[76] P. Ma, N. Flöry, Y. Salamin, et al., "Fast $MoTe_2$ waveguide photodetector with high sensitivity at telecommunication wavelengths," *ACS Photonics*, vol. 5, no. 5, pp. 1846–1852, 2018.
[77] J. F. Gonzalez Marin, D. Unuchek, K. Watanabe, T. Taniguchi, and A. Kis, "MoS_2 photodetectors integrated with photonic circuits," *NPJ 2D Mater. Appl.*, vol. 3, p. 14, 2019.
[78] N. Flöry, P. Ma, Y. Salamin, et al., "Waveguide-integrated van der Waals heterostructure photodetector at telecom wavelengths with high speed and high responsivity," *Nat. Nanotechnol.*, vol. 15, no. 2, pp. 118–124, 2020.
[79] G. Konstantatos, "Current status and technological prospect of photodetectors based on two-dimensional materials," *Nat. Commun.*, vol. 9, p. 5266, 2018.
[80] W. Hu, H. Cong, W. Huang, et al., "Germanium/perovskite heterostructure for high-performance and broadband photodetector from visible to infrared telecommunication band," *Light Sci. Appl.*, vol. 8, no. 11, p. 106, 2019.
[81] P. Norton, "HgCdTe infrared detectors," *Opto-Electron. Rev.*, vol. 10, no. 3, pp. 159–174, 2002.
[82] W. Lei, J. Antoszewski, and L. Faraone, "Progress, challenges, and opportunities for HgCdTe infrared materials and detectors," *Appl. Phys. Rev.*, vol. 2, no. 4, p. 041303, 2015.
[83] L. Prechtel, L. Song, S. Manus, D. Schuh, W. Wegscheider, and A. W. Holleitner, "Time-resolved picosecond photocurrents in contacted carbon nanotubes," *Nano Lett.*, vol. 11, no. 1, pp. 269–272, 2011.
[84] B. C. St-Antoine, D. Ménard, and R. Martel, "Single-walled carbon nanotube thermopile for broadband light detection," *Nano Lett.*, vol. 11, no. 2, pp. 609–613, 2011.
[85] M. Balestrieri, A.-S. Keita, E. Duran-Valdeiglesias, et al., "Polarization-sensitive single-wall carbon nanotubes all-in-one photodetecting and emitting device working at 1.55 μm," *Adv. Funct. Mater.*, vol. 27, no. 38, p. 170234, 2017.
[86] J. Clark and G. Lanzani, "Organic photonics for communications," *Nat. Photonics*, vol. 4, no. 7, pp. 438–446, 2010.
[87] K. Wada and L. C. Kimerling, *Photonics and Electronics with Germanium*, Weinheim, Germany, Wiley-VCH, 2015.
[88] S. Luryi, A. Kastalsky, and J. Bean, "New infrared detector on a silicon chip," *IEEE Trans. Electron Devices*, vol. 31, no. 9, pp. 1135–1139, 1984.
[89] E. Fitzgerald, Y. Xie, M. Green, et al., "Totally relaxed GeSi layers with low threading dislocation densities grown on Si substrates," *Appl. Phys. Lett.*, vol. 59, no. 7, pp. 811–814, 1991.
[90] M. T. Currie, S. B. Samavedam, T. A. Langdo, C. W. Leitz, and E. A. Fitzgerald, "Controlling threading dislocation densities in Ge on Si using graded SiGe layers and chemical-mechanical polishing," *Appl. Phys. Lett.*, vol. 72, no. 14, pp. 1718–1720, 1998.
[91] Y. Bogumilowicz, J. M. Hartmann, C. Di Nardo, et al., "High-temperature growth of very high germanium content SiGe virtual substrates," *J. Cryst. Growth*, vol. 290, no. 2, pp. 523–531, 2006.

[92] A. Rahim, J. Goyvaerts, B. Szelag, et al., "Open-access silicon photonics platforms in Europe," *IEEE J. Sel. Top. Quantum Electron.*, vol. 25, no. 5, p. 8200818, 2019.
[93] L. Colace, G. Masini, F. Galluzzi, and G. Assanto, "Metal–semiconductor–metal near-infrared light detector based on epitaxial Ge/Si," *Appl. Phys. Lett.*, vol. 72, no. 24, pp. 3175–3177, 1998.
[94] D. J. Eaglesham and M. Cerullo, "Low-temperature growth of Ge on Si(100)," *Appl. Phys. Lett.*, vol. 58, no. 20, pp. 2276–2278, 1991.
[95] H.-C. Luan, D. R. Lim, K. K. Lee, et al., "High-quality Ge epilayers on Si with low threading-dislocation densities," *Appl. Phys. Lett.*, vol. 75, no. 19, pp. 2909–2911, 1999.
[96] J. M. Hartmann, J.-F. Damlencourt, Y. Bogumilowicz, P. Holliger, G. Rolland, and T. Billon, "Reduced pressure-chemical vapor deposition of intrinsic and doped Ge layers on Si(0 0 1) for microelectronics and optoelectronics purposes," *J. Cryst. Growth*, vol. 274, nos 1–2, pp. 90–99, 2005.
[97] J. M. Hartmann, A. Abbadie, N. Cherkashin, H. Grampeix, and L. Clavelier, "Epitaxial growth of Ge thick layers on nominal and 6° off Si(0 0 1); Ge surface passivation by Si," *Semicond. Sci. Technol.*, vol. 24, no. 5, p. 055002, 2009.
[98] Z. Huang, J. Oh, and J. C. Campbell, "Back-side-illuminated high-speed Ge photodetector fabricated on Si substrate using thin SiGe buffer layers," *Appl. Phys. Lett.*, vol. 85, no. 15, pp. 3286–3288, 2004.
[99] J. Nakatsuru, H. Date, S. Mashiro, and M. Ikemoto, "Growth of high quality Ge epitaxial layer on Si(100) substrate using ultra thin Si0.5Ge0.5 buffer," Symposium EE – Progress in Semiconductor Materials V – Novel Materials and Electronics and Optoelectronic Applications, vol. 891, 2008.
[100] A. Nayfeh, C. O. Chui, and K. C. Saraswat, "Effects of hydrogen annealing on heteroepitaxial-Ge layers on Si: surface roughness and electrical quality," *Appl. Phys. Lett.*, vol. 85, no. 14, pp. 2815–2817, 2004.
[101] D. Choi, Y. Ge, J. S. Harris, J. Cagnon, and S. Stemmer, "Low surface roughness and threading dislocation density Ge growth on Si (0 0 1)," *J. Cryst. Growth*, vol. 310, no. 18, pp. 4273–4279, 2008.
[102] J. Osmond, G. Isella, D. Chrastina, R. Kaufmann, M. Acciarri, and H. von Känel, "Ultralow dark current Ge/Si(100) photodiodes with low thermal budget," *Appl. Phys. Lett.*, vol. 94, no. 2, p. 201106, 2009.
[103] V. Reboud, A. Gassenq, J. M. Hartmann, et al., "Germanium based photonic components toward a full silicon/germanium photonic platform," *Prog. Cryst. Growth Charact. Mater.*, vol. 63, no. 2, pp. 1–24, 2017.
[104] J. Ayala, J. Bell, K. Nummy, F. Guan, and S. Hum, "Integrating a high performance Germanium photodiode into a CMOS compatible flow for a full monolithic Silicon Photonics solution," in *IEEE 30th Annual SEMI Advanced Semiconductor Manufacturing Conference (ASMC)*, 2019, p. 18936046.
[105] Y. M. Haddara, P. Ashburn, and D. M. Bagnall, "Silicon-germanium: properties, growth and applications," in *Springer Handbook of Electronic and Photonic Materials*, S. Kasap, and P. Capper, Eds., Cham, Springer Handbooks. Springer, 2017.
[106] L. Virot, L. Vivien, J.-M. Fédéli, et al., "High-performance waveguide-integrated germanium PIN photodiodes for optical communication applications," *Photonics Res.*, vol. 1, no. 3, pp. 140–147, 2013.
[107] L. Colace, G. Masini, and G. Assanto, "Efficient high-speed near-infrared Ge photodetectors integrated on Si substrates," *Appl. Phys. Lett.*, vol. 76, no. 10, pp. 1231–1233, 2000.
[108] S. Famà, L. Colace, G. Masini, and G. Assanto, "High performance germanium-on-silicon detectors for optical communications," *Appl. Phys. Lett.*, vol. 81, no. 4, pp. 586–588, 2002.
[109] O. I. Dosunmu, D. D. Cannon, M. K. Emsley, L. C. Kimerling, and M. S. Ünlu, "High-speed resonant cavity enhanced Ge photodetectors on reflecting Si substrates for 1550-nm operation," *IEEE Photon. Technol. Lett.*, vol. 17, no. 1, pp. 175–177, 2005.
[110] M. Jutzi, M. Berroth, G. Wohl, M. Oehme, and E. Kasper, "Ge-on-Si vertical incidence photodiodes with 39-GHz bandwidth," *IEEE Photon. Technol. Lett.*, vol. 17, no. 7, pp. 1510–1512, 2005.
[111] J. Joo, S. Kim, I. G. Kim, K.-S. Jang, and G. Kim, "High-sensitivity 10 Gbps Ge-on-Si photoreceiver operating at λ ~1.55 μm," *Opt. Express*, vol. 18, no. 16, pp. 16474–16479, 2010.
[112] I. G. Kim, K.-S. Jang, J. Joo, et al., "High-performance photoreceivers based on vertical-illumination type Ge-on-Si photodetectors operating up to 43 Gb/s at λ~1550nm," *Opt. Express*, vol. 21, no. 25, pp. 30716–30723, 2013.
[113] D. Ahn, C.-Y. Hong, J. Liu, et al., "High performance, waveguide integrated Ge photodetectors," *Opt. Express*, vol. 15, no. 7, pp. 3916–3921, 2007.
[114] L. Vivien, M. Rouvière, J.-M. Fédéli, et al., "High speed and high responsivity germanium photodetector integrated in a Silicon-On-Insulator microwaveguide," *Opt. Express*, vol. 15, no. 15, pp. 9843–9848, 2007.
[115] T. Yin, R. Cohen, M. M. Morse, et al., "31GHz Ge n-i-p waveguide photodetectors on Silicon-on-Insulator substrate," *Opt. Express*, vol. 15, no. 21, pp. 13965–13971, 2007.
[116] G. Masini, S. Sahni, G. Capellini, J. Witzens, and C. Gunn, "High-speed near infrared optical receivers based on Ge waveguide photodetectors integrated in a CMOS process," *Adv. Opt. Technol.*, vol. 2008, p. 196572, 2008.
[117] L. Vivien, J. Osmond, J.-M. Fédéli, et al., "42 GHz p.i.n Germanium photodetector integrated in a silicon-on-insulator waveguide," *Opt. Express*, vol. 17, no. 8, pp. 6252–6257, 2009.
[118] S. Assefa, F. Xia, S. W. Bedell, et al., "CMOS-integrated high-speed MSM germanium waveguide photodetector," *Opt. Express*, vol. 18, no. 5, pp. 4986–4999, 2010.
[119] M. J. Byrd, E. Timurdogan, Z. Su, et al., "Mode-evolution-based coupler for high saturation power Ge-on-Si photodetectors," *Opt. Lett.*, vol. 42, no. 4, pp. 851–854, 2017.
[120] D. Ahn, L. C. Kimerling, and J. Michel, "Efficient evanescent wave coupling conditions for waveguide-integrated thin-film Si/Ge photodetectors on silicon-on-insulator/germanium-on-insulator substrates," *J. Appl. Phys.*, vol. 110, no. 8, p. 083115, 2011.
[121] L. Chen, P. Dong, and M. Lipson, "High performance germanium photodetectors integrated on submicron silicon waveguides by low temperature wafer bonding," *Opt. Express*, vol. 16, no. 15, pp. 11513–11518, 2008.
[122] H. Chen, P. Verheyen, P. De Heyn, et al., "–1 V bias 67 GHz bandwidth Si-contacted germanium waveguide p-i-n photodetector for optical links at 56 Gbps and beyond," *Opt. Express*, vol. 24, no. 5, pp. 4622–4631, 2016.

[123] D. J. Lockwood and L. Pavesi, *Silicon Photonics II Components and Integration*, Berlin and Heidelberg, Springer-Verlag, 2011.
[124] H. Wu, W. Luo, H. Zhou, M. Si, J. Zhang, and P. D. Ye, "First experimental demonstration of Ge 3D FinFET CMOS circuits," in *IEEE Symposium on VLSI Technology (VLSI Technology)*, 2015, pp. 58–59.
[125] J. Ayala, J. Bell, K. Nummy, F. Guan, and S. Hu, "Integrating a high performance Germanium photodiode into a CMOS compatible flow for a full monolithic Silicon Photonics solution," in *IEEE 30th Annual SEMI Advanced Semiconductor Manufacturing Conference (ASMC)*, 2019, pp. 1–4.
[126] B. Szelag, B. Blampey, T. Ferrotti, et al., "Multiple wavelength silicon photonic 200 mm R+D platform for 25Gb/s and above applications," in *Proc. SPIE 9891, Silicon Photonics and Photonic Integrated Circuits V*, p. 98911C, 2016.
[127] K. Giewont, K. A. Nummy, F. A. Anderson, et al., "300-mm monolithic silicon photonics foundry technology," *IEEE J. Sel. Top. Quantum Electron*, vol. 25, no. 5, p. 8200611, 2019.
[128] A. E.-J. Lim, J. Song, Q. Fang, et al., "Review of silicon photonics foundry efforts," *IEEE J. Sel. Top. Quantum Electron.*, vol. 20, no. 4, p. 8300112, 2014.
[129] F. Boeuf, S. Cremer, E. Temporiti, et al., "Silicon photonics R&D and manufacturing on 300-mm wafer platform," *IEEE/OSA J. Light. Technol.*, vol. 34, no. 2, pp. 286–295, 2016.
[130] D. Knoll, S. Lischke, A. Awny, et al., "BiCMOS silicon photonics platform for fabrication of high-bandwidth electronic-photonic integrated circuits," in *IEEE 16th Topical Meeting on Silicon Monolithic Integrated Circuits in RF Systems (SiRF)*, 2016, pp. 49-49.
[131] S. Lischke, D. Knoll, M. H. Eissa, M. Kroh, A. Peczek, L. Zimmermann, and A. Awny, "Performance improvement of a monolithically integrated C-Band receiver enabled by an advanced photonic BiCMOS process," in *IEEE Bipolar/BiCMOS Circuits and Technology Meeting (BCTM)*, 2017, pp. 50–53.
[132] M. Pantouvaki, S. A. Srinivasan, Y. Ban, et al., "Active components for 50 Gb/s NRZ-OOK optical interconnects in a silicon photonics platform," *IEEE/OSA J. Light. Technol.*, vol. 35, no. 4, pp. 631–638, 2017.
[133] A. J. Zilkie, P. Srinivasan, A. Trita, et al., "Multi-micron silicon photonics platform for highly manufacturable and versatile photonic integrated circuits," *IEEE J. Sel. Top. Quantum Electron.*, vol. 25, no. 5, p. 8200713, 2019.
[134] T. Aalto, M. Cherchi, M. Harjanne, et al., "Open-access 3-μm SOI waveguide platform for dense photonic integrated circuits," *IEEE J. Sel. Top. Quantum Electron.*, vol. 25, no. 5, p. 8201109, 2019.
[135] H. Pan, S. Assefa, W. M. J. Green, et al., "High-speed receiver based on waveguide germanium photodetector wire-bonded to 90nm SOI CMOS amplifier," *Opt. Express*, vol. 20, no. 16, pp. 18145–18155, 2012.
[136] J. Kang, R. Zhang, M. Takenaka, and S. Takagi, "Dark current suppression for germanium metal-semiconductor-metal photodetector by plasma post-oxidation passivation," in *IEEE 10th International Conference on Group IV Photonics*, 2013, pp. 140–141.
[137] S. Assefa, F. Xia, and Y. A. Vlasov, "Reinventing germanium avalanche photodetector for nanophotonic on-chip optical interconnects," *Nature*, vol. 464, no. 7285, pp. 80–84, 2010.
[138] C. T. DeRose, D. C. Trotter, W. A. Zortman, et al., "Ultra compact 45 GHz CMOS compatible germanium waveguide photodiode with low dark current," *Opt. Express*, vol. 19, no. 25, pp. 24897–24904, 2011.
[139] L. Vivien, A. Polzer, D. Marris-Morini, et al., "Zero-bias 40Gbit/s germanium waveguide photodetector on silicon," *Opt. Express*, vol. 20, no. 2, pp. 1096–1101, 2012.
[140] G. Li, Y. Luo, X. Zheng, et al., "Improving CMOS-compatible germanium photodetectors," *Opt. Express*, vol. 20, no. 24, pp. 26345–26350, 2012.
[141] J. H. Nam, F. Afshinmanesh, D. Nam, et al., "Monolithic integration of germanium-on-insulator p-i-n photodetector on silicon," *Opt. Express*, vol. 23, no. 12, pp. 15816–15823, 2015.
[142] H. Zhou and Y. Sun, "Size reduction of Ge-on-Si photodetectors via a photonic bandgap," *Appl. Opt.*, vol. 57, no. 12, pp. 2962–2966, 2018.
[143] J. Cui and Z. Zhou, "High-performance Ge-on-Si photodetector with optimized DBR location," *Opt. Lett.*, vol. 42, no. 24, pp. 5141–5144, 2017.
[144] T.-Y. Liow, N. Duan, A. E.-J. Lim, X. Tu, M. Yu, and G.-Q. Lo, "Waveguide Ge/Si avalanche photodetector with a unique low-height-profile device structure," in *Optical Fiber Communication Conference*, Optical Society of America, 2014, p. M2G.6.
[145] Y. Zhang, S. Yang, Y. Yang, et al., "A high-responsivity photodetector absent metal-germanium direct contact," *Opt. Express*, vol. 22, no. 9, pp. 11367–11375, 2014.
[146] S. Lischke, D. Knoll, C. Mai, et al., "High bandwidth, high responsivity waveguide-coupled germanium p-i-n photodiode," *Opt. Express*, vol. 23, no. 21, pp. 27213–27220, 2015.
[147] H. T. Chen, P. Verheyen, P. De Heyn, et al., "High-responsivity low-voltage 28-Gb/s Ge p-i-n photodetector with silicon contacts," *IEEE/OSA J. Light. Technol*, vol. 33, no. 4, pp. 820–824, 2015.
[148] H. Chen, M. Galili, P. Verheyen, et al., "100-Gbps RZ data reception in 67-GHz Si-contacted germanium waveguide p-i-n photodetectors," *IEEE/OSA J. Light. Technol.*, vol. 35, no. 4, pp. 722–726, 2017.
[149] J. Lambrecht, H. Ramon, B. Moeneclaey, et al., "90-Gb/s NRZ optical receiver in silicon using a fully differential transimpedance amplifier," *IEEE/OSA J. Light. Technol.*, vol. 37, no. 9, pp. 1964–1973, 2019.
[150] L. Virot, D. Benedikovic, B. Szelag, et al., "Integrated waveguide PIN photodiodes exploiting lateral Si/Ge/Si heterojunction," *Opt. Express*, vol. 25, no. 16, pp. 19487–19496, 2017.
[151] D. Benedikovic, L. Virot, G. Aubin, et al., "25 Gbps low-voltage hetero-structured silicon-germanium waveguide pin photodetectors for monolithic on-chip nanophotonic architectures," *Photon. Res.*, vol. 7, no. 4, pp. 437–444, 2019.
[152] D. Benedikovic, L. Virot, G. Aubin, et al., "Comprehensive study on chip-integrated germanium pin photodetectors for energy-efficient silicon interconnects," *IEEE J. Quantum Electron.*, vol. 56, no. 1, p. 8400409, 2020.
[153] G. P. Agrawal, *Fiber-Optics Telecommunication Systems*, 3rd ed., New York, Wiley-Interscience, 2002.
[154] Y. Kang, H.-D. Liu, M. Morse, et al., "Monolithic germanium/silicon avalanche photodiodes with 340 GHz gain–bandwidth product," *Nat. Photonics*, vol. 3, no. 59, pp. 59–63, 2009.

[155] W. S. Zaoui, H.-W. Chen, J. E. Bowers, et al., "Frequency response and bandwidth enhancement in Ge/Si avalanche photodiodes with over 840GHz gain-bandwidth-product," *Opt. Express*, vol. 17, no. 15, pp. 2641–12649, 2009.
[156] N. Duan, T.-Y. Liow, A. E.-J. Lim, L. Ding, and G. Q. Lo, "310 GHz gain-bandwidth product Ge/Si avalanche photodetector for 1550 nm light detection," *Opt. Express*, vol. 20, no. 10, pp. 11031–11036, 2012.
[157] L. Virot, P. Crozat, J.-M. Fédéli, et al., "Germanium avalanche receiver for low power interconnects," *Nat. Commun.*, vol. 5, p. 4957, 2014.
[158] H. T. Chen, J. Verbist, P. Verheyen, et al., "High sensitivity 10Gb/s Si photonic receiver based on a low-voltage waveguide-coupled Ge avalanche photodetector," *Opt. Express*, vol. 23, no. 2, pp. 815–822, 2015.
[159] N. J. D. Martinez, C. T. Derose, R. W. Brock, et al., "High performance waveguide-coupled Ge-on-Si linear mode avalanche photodiodes," *Opt. Express*, vol. 24, no. 17, pp. 19072–19081, 2016.
[160] H. T. Chen, J. Verbist, P. Verheyen, et al., "25-Gb/s 1310-nm optical receiver based on a sub-5-V waveguide-coupled germanium avalanche photodiode," *IEEE Photonics J.*, vol. 7, no. 4, p. 7902909, 2015.
[161] Z. Huang, C. Li, D. Liang, et al., "25 Gbps low-voltage waveguide Si–Ge avalanche photodiode," *Optica*, vol. 3, no. 8, pp. 793–798, 2016.
[162] X. Zeng, Z. Huang, B. Wang, D. Liang, M. Fiorentino, and R. G. Beausoleil, "Silicon–germanium avalanche photodiodes with direct control of electric field in charge multiplication region," *Optica*, vol. 6, no. 6, pp. 772–777, 2019.
[163] B. Wang, Z. Huang, Y. Yuan, et al., "64 Gb/s low-voltage waveguide SiGe avalanche photodiodes with distributed Bragg reflectors," *Photonics Res.*, vol. 8, no. 7, pp. 1118–1123, 2020.
[164] B. Wang, Z. Huang, W. V. Sorin, et al., "A low-voltage Si-Ge avalanche photodiode for high-speed and energy efficient silicon photonic links," *IEEE/OSA J. Light. Technol.*, vol. 38, no. 12, pp. 3156–3163, 2020.
[165] A. Samani, O. Carpentier, E. El-Fiky, et al., "Highly sensitive, 112 Gb/s O-band waveguide coupled silicon-germanium avalanche photodetectors," in *Optical Fiber Communication Conference*, Optical Society of America, 2019, p. Th3B.1.
[166] O. Carpentier, A. Samani, M. Jacques, et al., "High gain-bandwidth waveguide coupled silicon germanium avalanche photodiode," in *Conference on Lasers and Electro-Optics*, Optical Society of America, 2020, p. STh4O.3.
[167] M. Huang, P. Cai, S. Li, et al., "Breakthrough of 25Gb/s germanium on silicon avalanche photodiode," in *Optical Fiber Communication Conference*, Optical Society of America, 2016, p. Tu2D.2.
[168] M. Huang, P. Cai, S. Li, et al., "56GHz waveguide Ge/Si avalanche photodiode," in *Optical Fiber Communication Conference*, Optical Society of America, 2018, p. W4D.6.
[169] G. Kim, S. Kim, S. A. Kim, J. H. Oh, and K.-S. Jang, "NDR-effect vertical-illumination-type Ge-on-Si avalanche photodetector," *Opt. Lett.*, vol. 43, no. 22, pp. 5583–5586, 2018.
[170] D. Benedikovic, L. Virot, G. Aubin, et al., "40 Gbps heterostructure germanium avalanche photo receiver on a silicon chip," *Optica*, vol. 7, no. 7, pp. 775–783, 2020.
[171] S. Park, Y. Malinge, O. Dosunmu, et al., "50-Gbps receiver subsystem using Ge/Si avalanche photodiode and integrated bypass capacitor," in *Optical Fiber Communication Conference*, Optical Society of America, 2019, p. M3A.3.
[172] S. A. Srinivasan, J. Lambrecht, M. Berciano, et al., "Highly sensitive 56 Gbps NRZ O-band BiCMOS-silicon photonics receiver using a Ge/Si avalanche photodiode," in *Optical Fiber Communication Conference*, Optical Society of America, 2020, p. W4G.7.
[173] Y. Guo, Y. Yin, Y. Song, et al., "Demonstration of 25Gbit/s per channel NRZ transmission with 35 dB power budget using 25G Ge/Si APD for next generation 100G-PON," in *Optical Fiber Communication Conference*, Optical Society of America, 2017.p. M3H.6.
[174] J. C. Campbell, "Recent advances in avalanche photodiodes," *IEEE/OSA J. Light. Technol.*, vol. 34, no. 2, pp. 278–285, 2016.
[175] M. Huang, S. Li, P. Cai, et al., "Germanium on silicon avalanche photodiode," *IEEE J. Sel. Top. Quantum Electron.*, vol. 24, no. 2, p. 3800911, 2018.
[176] S. A. Srinivasan, M. Berciano, P. De Heyn, S. Lardenois, M. Pantouvaki, and J Van Campenhout, "27 GHz silicon-contacted waveguide-coupled Ge/Si avalanche photodiode," *IEEE/OSA J. Light. Technol.*, vol. 38, no. 11, pp. 3044–3050, 2020.
[177] J. Verbist, J. Lambrecht, B. Moeneclaey, et al., "40-Gb/s PAM-4 transmission over a 40 km amplifier-less link using a sub-5V Ge APD," *IEEE Photon. Technol. Lett.*, vol. 29, no. 24, pp. 2238–2241, 2017.
[178] B. Wang, Z. Huang, X. Zeng, et al., "50 Gb/s PAM4 low-voltage Si-Ge avalanche photodiode," in *Optical Fiber Communication Conference*, Optical Society of America, 2020, p. SM4J.7.
[179] Y. Yuan, Z. Huang, B. Wang, et al., "Superior temperature performance of Si-Ge waveguide avalanche photodiodes at 64Gbps PAM4 operation," in *Optical Fiber Communication Conference*, Optical Society of America, 2020, p. M2A.2.
[180] Z. Huang, B. Wang, Y. Yuan, D. Liang, M. Fiorentino, and R. G. Beausoleil, "64Gbps PAM4 modulation for a low energy Si-Ge waveguide APD with distributed Bragg reflectors," in *Optical Fiber Communication Conference*, Optical Society of America, 2020, p. W4G.8.
[181] M. Ware, K. Rajamani, M. Floyd, et al., "Architecting for power management: the IBM POWER7 approach," in *International Symposium on High Performance Computer Architecture (HPCA)*, IEEE, 2010, pp. 1–11.
[182] P. Vines, K. Kuzmenko, J. Kirdoda, et al., "High performance planar germanium-on-silicon single-photon avalanche diode detectors," *Nat. Commun.*, vol. 10, p. 1086, 2019.
[183] R. E. Warburton, G. Intermite, M. Myronov, et al., "Ge-on-Si single-photon avalanche diode detectors: design, modeling, fabrication, and characterization at wavelengths 1310 and 1550 nm," *IEEE Trans. Electron Devices*, vol. 60, no. 11, pp. 3807–3813, 2013.
[184] A. Sammak, M. Aminian, L. K. Nanver, and E. Charbon, "CMOS-compatible pure GaB Ge-on-Si APD pixel arrays," *IEEE Trans. Electron Devices*, vol. 63, no. 1, pp. 92–99, 2016.
[185] Y. Li, X. Luo, G. Liang, and G.-Q. Lo, "Demonstration of Ge/Si avalanche photodetector arrays for lidar application," in *Optical Fiber Communication Conference*, Optical Society of America, 2019, p. Tu3E.3.
[186] J. D. Petticrew, S. J. Dimler, X. Zhou, A. P. Morrison, C. H. Tan, and J. S. Ng, "Avalanche breakdown timing statistics for silicon single photon avalanche diodes," *IEEE J. Sel. Top. Quantum Electron.*, vol. 24, no. 2, p. 3801506, 2018.

[187] M.-J. Lee, P. Sun, G. Pandraud, C. Bruschini, and E. Charbon, "First near-ultraviolet- and blue-enhanced backside-illuminated single-photon avalanche diode based on standard SOI CMOS technology," *IEEE J. Sel. Top. Quantum Electron.*, vol. 25, no. 5, p. 3800206, 2019.

[188] J. Zhang, M. A. Itzler, H. Zbinden, and J.-W. Panm, "Advances in InGaAs/InP single-photon detector systems for quantum communication," *Light Sci. Appl.*, vol. 4, p. e286, 2015.

[189] D. Marpaung, J. Yao, and J. Capmany, "Integrated microwave photonics," *Nat. Photonics*, vol. 13, no. 2, pp. 80–90, 2019.

[190] V. J. Urick, J. D. Mckinney, and K. J. Williams, *Fundamentals of Microwave Photonics*, Hoboken, New Jersey, John Wiley & Sons, 2015.

[191] A. Ramaswamy, M. Piels, N. Nunoya, T. Yin, and J. E. Bowers, "High power silicon-germanium photodiodes for microwave photonic applications," *IEEE Trans. Microw. Theory Tech.*, vol. 58, no. 11, pp. 3336–3343, 2010.

[192] A. Beling, X. Xie, and J. C. Campbell, "High-power, high-linearity photodiodes," *Optica*, vol. 3, no. 3, pp. 328–338, 2016.

[193] T.-C. Tzu, K. Su, R. Costanzo, D. Ayoub, S. M. Bowers, and A. Beling, "Foundry-enabled high-power photodetectors for microwave photonics," *IEEE J. Sel. Top. Quantum Electron.*, vol. 25, no. 5, p. 3800111, 2019.

[194] X. Li, L. Peng, Z. Liu, et al., "High-power back-to-back dual-absorption germanium photodetector," *Opt. Lett.*, vol. 45, no. 6, pp. 1358–1361, 2020.

[195] Y. Zuo, Y. YU, Y Zhang, D. Zhou, and X. Zhang, "Integrated high-power germanium photodetectors assisted by light field manipulation," *Opt. Lett.*, vol. 44, no. 13, pp. 3338–3341, 2019.

[196] C.-M. Chang, J. H. Sinsky, P. Dong, G. de Valicourt, and Y.-K. Chen, "High-power dual-fed traveling wave photodetector circuits in silicon photonics," *Opt. Express*, vol. 23, no. 17, pp. 22857–22866, 2015.

[197] L. Bogaert, K. Van Gasse, T. Spuesens, G. Torfs, J. Bauwelinck, and G. Roelkens, "Silicon photonics traveling wave photodiode with integrated star coupler for high-linearity mm-wave applications," *Opt. Express*, vol. 26, no. 26, pp. 34763–34775, 2018.

[198] Z. Fu, H. Yu, Q. Zhang, X. Wang, P. Xia, and J. Yang, "High-power traveling-wave photodetector based on an aperiodically loaded open-circuit electrode," *Opt. Lett.*, vol. 44, no. 22, pp. 5582–5585, 2019.

[199] R. Soref, "Emerging SiGeSn integrated-photonics technology," in *IEEE Photonics Society Summer Topical Meeting Series*, 2016, p. TuA1.3.

[200] D. J. Richardson, "Filling the light pipe," *Science*, vol. 330, no. 6002, pp. 327–328, 2010.

[201] F. Gunning and B. Corbett, "Time to open the 2-μm window?," *Optic Photonics News*, vol. 30, no. 3, pp. 42–47, 2019.

[202] H. Ono, J. Fujikata, M. Noguchi, et al., "Si photonics butt-coupled waveguide germanium avalanche photodiodes with lateral SAM structures," in *Optical Fiber Communication Conference*, Optical Society of America, 2019, p. Th2A.9.

[203] Z. Su, E. S. Hosseini, E. Timurdogan, et al., "Whispering gallery germanium-on-silicon photodetector," *Opt. Lett.*, vol. 42, no. 15, pp. 2878–2881, 2017.

[204] Y.-H. Huang, G.-E. Chang, H. Li, and H. H. Cheng, "Sn-based waveguide p-i-n photodetector with strained GeSn/Ge multiple-quantum-well active layer," *Opt. Lett.*, vol. 42, no. 9, pp. 1652–1655, 2017.

[205] Y. Dong, W. Wang, S. Xu, et al., "Two-micron-wavelength germanium-tin photodiodes with low dark current and gigahertz bandwidth," *Opt. Express*, vol. 25, no. 14, pp. 15818–15827, 2017.

[206] S. Xu, W. Wang, Y.-C. Huang, et al., "High-speed photo detection at two-micron-wavelength: technology enablement by GeSn/Ge multiple-quantum-well photodiode on 300 mm Si substrate," *Opt. Express*, vol. 27, no. 4, pp. 5798–5813, 2019.

[207] C.-H. Tsai, B.-J. Huang, R. A. Soref, G. Sun, H. H. Cheng, and G.-E. Chang, "GeSn resonant-cavity-enhanced photodetectors for efficient photodetection at the 2 μm wavelength band," *Opt. Lett.*, vol. 45, no. 6, pp. 1463–1466, 2020.

[208] Y. Lin, D. Ma, R.-T. Wen, et al., "Germanium photodetectors with 60-nm absorption coverage extension and ~2× quantum efficiency enhancement across L-band," in *IEEE 16th International Conference on Group IV Photonics (GFP)*, 2019.

[209] K. Takeda, T. Hiraki, T. Tsuchizawa, et al., "Contributions of Franz–Keldysh and avalanche effects to responsivity of a germanium waveguide photodiode in the L-band," *IEEE J. Sel. Top. Quantum Electron.*, vol. 20, no. 4, p. 3800507, 2014.

[210] T.-Y. Liow, A. E.-J. Lim, N. Duan, M. Yu, and G.-Q. Lo, "Waveguide germanium photodetector with high bandwidth and high L-band responsivity," in *Optical Fiber Communication Conference/National Fiber Optic Engineers Conference*, Optical Society of America, 2013, p. OM3K.2.

[211] R. Anthony, D. E. Hagan, D. Genuth-Okon, et al., "Extended wavelength responsivity of a germanium photodetector integrated with a silicon waveguide exploiting the indirect transition," *IEEE J. Sel. Top. Quantum Electron.*, vol. 26, no. 2, p. 3800107, 2020.

[212] Z. Zhao, C. Ho, Q. Li, K. Toprasertpong, S. Takagi, and M. Takenaka, "Monolithic germanium PIN waveguide photodetector operating at 2 μm wavelengths," in *Optical Fiber Communication Conference*, Optical Society of America, 2020, p. W4G.3.

[213] X. Y. Li, J. Y. Wang, Y. F. Liu, et al., "Design of Ge1-xSnx-on-Si waveguide photodetectors featuring high-speed high-sensitivity photodetection in the C- to U-bands," *Appl. Opt.*, vol. 59, no. 25, pp. 7646–7651, 2020.

[214] H. Tran, T. Pham, J. Margetis, et al., "Si-based GeSn photodetectors toward mid-infrared imaging applications," *ACS Photonics*, vol. 6, no. 11, pp. 2807–2815, 2019.

[215] S. Xu, Y.-C. Huang, S. Masudy-Panah, X. Gong, and Y.-C. Yeo, "Enhanced photo response at two-micron-wavelength using GeSn/Ge multiple-quantum-well waveguide," in *Optical Fiber Communication Conference*, Optical Society of America, 2019, p. STu4J.1.

[216] S. Xu, K. Han, Y.-C. Huang, et al., "Integrating GeSn photodiode on a 200 mm Ge-on-insulator photonics platform with Ge CMOS devices for advanced OEIC operating at 2 μm band," *Opt. Express*, vol. 27, no. 19, pp. 26924–26939, 2019.

[217] H. Zhou, S. Xu, Y. Lin, et al., "High-efficiency GeSn/Ge multiple-quantum-well photodetectors with photon-trapping microstructures operating at 2 μm," *Opt. Express*, vol. 28, no. 7, pp. 10280–10293, 2020.

[218] W. Wang, Y. Dong, S.-Y. Lee, et al., "Floating-base germanium-tin heterojunction phototransistor for

high-efficiency photodetection in short-wave infrared range," *Opt. Express*, vol. 25, no. 16, pp. 18502–18507, 2017.

[219] W.-T. Hung, D. Barshilia, R. Basu, H. H. Cheng, and G.-E. Chang, "Silicon-based high-responsivity GeSn short-wave infrared heterojunction phototransistors with a floating base," *Opt. Lett.*, vol. 45, no. 5, pp. 1088–1091, 2020.

[220] Y. Dong, W. Wang, S. Y. Lee, et al., "Germanium-tin multiple quantum well on silicon avalanche photodiode for photodetection at two micron wavelength," *Semicond. Sci. Technol.*, vol. 31, no. 9, p. 095001, 2016.

[221] H. Tran, T. Pham, J. Margetis, et al., "Si-based GeSn photodetectors toward mid-infrared imaging applications," *ACS Photonics*, vol. 6, no. 11, pp. 2807–2815, 2019.